

Equilibrium Time, Permutation, Multiscale and Modified Multiscale Entropies for Low-High Infection Level Intracellular Viral Reaction Kinetics

Farid Taherkhani (✉ faridtaherkhani@gmail.com)

Universität Bremen: Universitat Bremen

Research Article

Keywords: Permutation Entropy, Multi Scale Entropy, Kinetics Monte Carlo, Equilibrium Time, Intracellular Viral Reaction

Posted Date: March 9th, 2021

DOI: <https://doi.org/10.21203/rs.3.rs-235645/v1>

License:  This work is licensed under a Creative Commons Attribution 4.0 International License.

[Read Full License](#)

**Equilibrium Time, Permutation, Multiscale and Modified Multiscale
Entropies for Low-High Infection Level Intracellular Viral Reaction
Kinetics**

Farid Taherkhani^{*}

Departments of Production Engineering University of Bremen, Germany

Corresponding Author:
faridtaherkhani@gmail.com

Abstract

Kinetics Monte Carlo simulation has been done for solving Master equation for intracellular viral reaction kinetics. There is scaling relationship between reaction equilibrium time and initial population of template species in intracellular viral reaction kinetics. Kinetics Monte Carlo result shows that mathematical presentation between initial population of template species and reaction equilibrium time is $f_{eq\ time}(N) = aN^b$ ($a = 163.1$, $b = -0.1429$), where N , $f_{eq\ time}(N)$ are initial population of template species and reaction equilibrium time respectively. Kinetics Monte Carlo shows that increasing initial population of template species decreases the reaction equilibrium time. Initial population for template species with range $1 \leq \text{Temp} \leq 4$; $\text{Temp}=5$; $6 \leq \text{Temp} \leq 10$ are called low, medium and high infection level in intracellular viral kinetics reaction respectively. Entropy generation has been considered in low, intermediate and high infection level of intracellular viral reaction kinetics in during dynamical population. Permutation, multiscaling and modified multiscaling entropies have been calculated for species, genome, structural protein, and template species. Dependency of permutation entropy on permutation order is small in high infection level. At short time scale, convergency of permutation entropy occurs with medium permutation order value. In the big time scale, permutation entropy $H(n)$ scales with permutation order n as a scaling relation $H(n) = n^\alpha$ ($\alpha=0.30$). Three different trends for low, medium and high infection level observed for multiscaling entropy of template species versus scaling factor. Non-monotonic behavior for permutation entropy versus time could be observed for structural protein species.

Keyword: Permutation Entropy, Multi Scale Entropy, Kinetics Monte Carlo, Equilibrium Time, Intracellular Viral Reaction

1. Introduction

Lyapunov exponent, entropy and fractal dimension are essential parameters which are so useful for recognition chaotic, random and complex time series data analysis [6,13].

Many computer algorithms, numerical and mathematical methods have been developed for complexity measure for noisy, chaotic and random data in past 20 years ago. During the last three decades many interesting methods has been proposed for investigation vibrational and dynamical changes based on analyzing metric of nearest neighbors in phase space method [10]. Analyzing vibrational and dynamical changes of data based on nearest neighbors in phase space method is very calculation consuming time [10].

Permutation entropy is presented as a very effective and fast method for complexity measure and analyzing chaotic time series data and for analyzing speech signal.

Permutation entropy for analyzing of time series of heart interbeat signal has been applied for recognition healthy and heart failure people[15].

Due to regular working of heart interbeat signal of sick person, permutation entropy of healthy people is higher than those sick person [15].

Pathologies such as cardiac arrhythmias like atrial fibrillation are related to the high statistical fluctuation and uncorrelated noise [19,8,9].

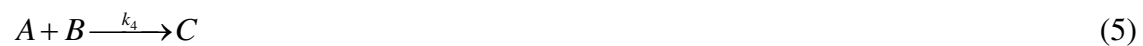
A virus is made up of a core of genetic material, either DNA or RNA, surrounded by a protective coat called a capsid. Computer programming could explain many complexities behavior of living cells [9].

Our aim of work is understanding of complexity of dynamics of intracellular dynamics help us to predict the behavior of viruses in during of growth process. Entropy value in during time evolution for dynamical of complex bio-chemical reaction will be explored.

Natural complexity of intracellular reaction dynamics in low-high infection level will be examined with different entropy approach and ability of them for recognition dynamical complexity. Initial population of template effect on entropy trend in during dynamical process will be explored. We will investigate reaction equilibrium time as function of initial population of template.

2. Intracellular Viral Kinetics

The Viral nucleic acids were classified as genomic (gen) or template (temp). The genome may be DNA and RNA which are positive- strand, negative strand or some other type. According to equations (1-5) we have two ways for changing the genome. The first way, the genome converts to template which has catalytic role for synthesizing every Viral component[14]. The second way it packages within structural proteins to form progeny virus with different probabilities. It is very important to notice that the synthesis of structural protein requires that the Viral DNA be transcribed to mRNA and mRNA must be translated to generate the structural protein. At first when the population of template is very high structural protein is synthesized for incorporation into progeny particle. We can show the mechanism of viral kinetics according following reaction:[14]



In this mechanism A, B, C, D, E and X are genome, structural protein, virus, degradation template, degradation or secretion, and template, respectively.

The rate constant and initial molecular populations are taken from reference as a following Table [14]

Rate Constant	$k_1 = .025$ day ⁻¹	$k_2 = .25$ day ⁻¹	$k_3 = 1$ day ⁻¹	$k_4 = 0.0000075$ molecules ⁻¹ day ⁻¹	$k_5 = 1000$ day ⁻¹	$k_6 = 1.99$ day ⁻¹
Initial population	$A = 10$	$B = 0$	$C = 0$	$D = 0$	$E = 0$	$X = 1$

Rate constant in dynamical system in random media is a function of time and rate constant can be related to the Fisher information and increasing the reaction order can increase or decrease dynamical disorder [11].

2. Theoretical background

2.1. Stochastic Algorithm and Simulation

Another way to investigate the kinetics of a small system is stochastic simulation. Up to now several authors have applied the stochastic algorithms [7]. In recent years stochastic modeling has been emerged as a physically more realistic alternative for modeling of the vivo reactions[7,17,16]. Stochastic and random diffusion model can be described for autocatalytic reaction model such as Lotka-Volterra reaction-diffusion or predator-prey system [1]. Let X be the time of the event. By a constant hazard we mean that:

$$P(X \in (t, t + dt] | X > t) = \alpha dt \quad (6)$$

where $\alpha > 0$ is a constant whose value may be calculated as, $\alpha = \sum_{i=1}^M W_{j,n} = \sum_{i=1}^M \alpha_i$, where

$$\alpha_i = W_{j,n} = k_i \frac{j!}{n!(j-n)!}, \quad k \text{ is a rate constant. For a small } \delta t \text{ we will have:}$$

$$P(X \in (t, t + dt) | X > t) = \alpha \delta t \quad (7)$$

Considering a time $t > 0$, and a large integer N , dividing the interval $(0, t]$ into N

subintervals of the form $((i-1)\delta t, i\delta t], i=1,2,\dots,N$ where $\delta t = \frac{t}{N}$, then we have:

$$P(X > t) = P[X \notin (0, t)] = P[\{(X \notin (0, \delta t)) \text{I } \{X \notin (\delta t, 2\delta t)\} \text{I } \dots \{X \notin (N-1)\delta t, t\}\}] \quad (8)$$

Hence

$$\begin{aligned} P(X > t) &= P(X \notin (0, \delta t])P(X \notin (\delta t, 2\delta t] | X > \delta t) \\ &\dots P(X \notin ((N-1)\delta t, t] | X > (N-1)\delta t) \\ &\approx (1 - \alpha \delta t) \times (1 - \alpha \delta t) \times \dots (1 - \alpha \delta t) = \\ &(1 - \alpha \delta t)^N \\ &= \left(1 - \frac{\alpha t}{N}\right)^N \end{aligned} \quad (9)$$

If $N \rightarrow \infty$ and $\delta t \rightarrow 0$ therefore equation 9 will convert to $\exp(-\alpha t)$ then

$P(X \leq t) = (1 - \exp(-\alpha t))$. Consequently, whenever we consider a time dependent event with constant hazard α , in Gillespie algorithm[7]. We can conclude that the time distribution is an exponential function. By choosing two uniform random numbers and within the interval $[0, 1]$ and by definition of two following expressions, we may write:

$$\tau = \frac{1}{\alpha} \ln\left(\frac{1}{r_1}\right) \quad (10)$$

$$\sum_{i=1}^{\mu-1} \alpha_i < r_2 \alpha \leq \sum_{i=1}^{\mu} \alpha_i \quad (11)$$

There are three loops for algorithm as follows:

1) Calculating $\alpha_i = k_i \frac{j!}{n!(j-n)!}$, whereas k is a rate constant. For $1 \leq \mu \leq M$

2) Generating two uniform random numbers r_1 and r_2 and calculating τ and μ according to equations 10 and 11.

3) Increasing t by τ and adjusting population of reactants for reaction μ [7]

2.2. Permutation Entropy

Permutation entropy for time series as $(x(i), i=1, 2, \dots)$ is defined as the Shannon entropy for k distinct symbols:

$$H_p(n) = - \sum_{j=1}^k P_j \ln(P_j) \quad (12)$$

When $P_j = \frac{1}{n!}$, then $H_p(n)$ attain the maximum value $\ln(n!)$ [2,15]. For convenience,

we always normalized:

$$0 \leq \frac{H_p(n)}{\ln(n!)} \leq 1 \quad (13)$$

We can define the permutation entropy per symbol [15,3] of order n

$$h_n = \frac{H(n)}{n-1} \quad (14)$$

In our calculation the order of permutation entropy is taken $n=4$.

2.3 . Multiscaling Entropy

Another approach for investigation of complexity of biological signal is multiscaling entropy. Given a one-dimensional discrete time series, $\{x_1, \dots, x_i, \dots, x_N\}$, Madalena et.al. construct consecutive coarse-grained time series, $\{y^{(\tau)}\}$ determined by the scale factor τ

according to the equation $y_j^{(\tau)} = \frac{1}{\tau} \sum_{i=(j-1)\tau+1}^{j\tau} x_i$. For scale one, the time series $\{y^{(1)}\}$ is

simply the original time series. The length of each coarse-grained time series is equal to the length of the original time series divided by the scale factor τ . Madalena et.al. then calculate an entropy measure for each coarse grained time series plotted as a function of the scale factor τ [4,5,12]. Madalena et.al. called this procedure multiscale entropy (MSE) analysis[5].

3. Result and discussion

Preprint of modified current paper could be found at references [18].

3.1. Reaction equilibrium time of viral kinetics model as a function of template number:

Kinetics Monte Carlo approach is used for simulation of intracellular viral reaction kinetics via Gillespie algorithm. Stochastic dynamics for investigation number of template particle is investigated as a function of time. Reaction equilibrium time after 1000 times of stochastic simulation is obtained as a function of initial template population.

On the basis of Figure 1 there is scaling relation between the reaction equilibrium of time and the number of template particle. Fitting of Figure 1 with function $f_{eq\ time}(N) = aN^b$ shows $a = 163.1$, $b = -0.1429$ and R square = 0.9844. On the basis of Fig.1. result of kinetics Monte Carlo shows that with increasing the number of template species, reaction equilibrium of time decreases with initial template species as a power law. Equation $f_{eq\ time}(N) = aN^b$ shows that reaction equilibrium time decreases very fast for the great initial number of template species. Figure 1 shows reaction equilibrium time for large

number of template species is small. Owing to this fact, increasing the number of template species decreases the fluctuation population of template, then system approaches to stationary state at the short time.

3.2. Permutation entropy Result

Stochastic simulations have been done for intracellular viral reaction kinetics via Gillespie algorithm. Poisson algorithms could be used for stochastic simulation of chemical master equation as well. Population of structural protein, genome and template species has been calculated as a function of time. Schematic presentation for population dynamics of genome, structural protein species with Gillespie and Poisson algorithms are shown in Figure 2.a and Fig.2.b respectively. Based on equations 12, 14, permutation entropy versus time has been calculated for stochastic population species in intracellular viral reaction kinetics.

Stochastic simulation has been done for 1000 independent runs for genome, template and structural protein species and in each run permutation entropy has been calculated.

Therefore, average of 1000 permutation entropy in each run versus time is computed.

Infection level in intracellular reaction is defined based on initial population of template (Temp) species. Initial population for template species with range

$1 \leq \text{Temp} \leq 4$; $\text{Temp}=5$; $6 \leq \text{Temp} \leq 10$ are called low, medium and high infection level intracellular viral kinetics reaction respectively.

Average of 1000 independent permutation entropy calculation from kinetic Monte Carlo result in during 200 days for genome species in low and high infection, is shown in Figure4.a. On the basis of Figure.4.a in low simulation time, permutation entropy of genome species in low-high infection level is smaller than high infection level .

Permutation entropy trend is reversed with initial template population $Temp > 5$ in big time for order permutation $n=4$. For big permutation entropy order $n=6$ permutation entropy increases with the initial template population monotonically. Result of permutation entropy from averaging of 1000 independent permutation entropy from kinetics Monte Carlo population trajectory as a function of time for structural protein with initial population number $Temp = 2,3$ and $Temp = 5-7$ are presented at Figure.4.b and Figure.4.c respectively. On the basis of Figure.4.b in low infection level of intracellular viral reaction kinetics, there are two peaks as a sharp and wide in short time scale, finally permutation entropy for structural protein decreases in large time scale linearly. One peak is observed for permutation entropy of structural protein in high infection level in small time scale.

Permutation entropy trend for structural protein species is linear in big time scale.

Permutation entropy has been calculated for template species dynamics in low and high infection level. Result of permutation entropy of template species has been presented at Figure.4.d. On the basis of Figure.4.d. permutation entropy of template species increases with infection level.

Result of permutation entropy as a function of time with three permutation order, $n=2, 4, 6$ for low and high infection level has been shown in Figure.5.a,b respectively. On the basis of permutation entropy result at Figure.5.a and Figure5.b, with increasing infection level convergency of permutation entropy occurs with the low permutation order (n).

Convergency of permutation entropy has been tested on windows and permutation order (n) values. Dependency of permutation entropy on order and windows value at ($n=4$, windows=512) and ($n=6$, windows=1024) are presented at Figure.5.c and Figure.5.d

respectively. On the basis of Figure.5.c and Figure.5.d the windows value on permutation entropy at high permutation order ($n=6$), is so small. Generally, permutation entropy convergency occurs on permutation order for $n>6$. Permutation entropy calculation shows that at short time scale convergency occurs with medium value of permutation order but by passing time dynamical permutation entropy depend on n value and in big time scale permutation entropy shows as a scaling law $H(n) = n^\alpha$ ($\alpha=0.30$). Fitting result for permutation entropy with order permutation, n , has been presented at Figure.5.e.

Comparison of permutation entropy for three kinds of species such as structural protein, template and genome based on five initial template numbers are presented at Figure.6.a and Figure.6.b respectively. On the basis of Figures.6 permutation entropy versus time (day) has a following order: template > structural protein > genome.

Noise effect has been investigated on permutation entropy for stochastic dynamics of intracellular reaction kinetics. Permutation entropy result at high infection level in absence and presence of noise in dynamical intracellular reaction is shown in Figure.6.c and Figure.6.d respectively. On the basis of Figure.6.c and Figure.6.d including noise in population dynamics, permutation entropy result will be changed. Owing to this fact noise can change the entropy value and magnitude order entropy for genome, template and structural protein species. Including noise in permutation entropy is not able to predict the complexity of stochastic dynamics of intracellular viral reaction. Our result shows that presence of noise in dynamical process of intracellular viral reaction will change order of permutation entropy for the mentioned of three species. Permutation entropy in presence chaotic noise has the following order template > genome > structural protein. In absence of noise permutation entropy value has a different order such as

structural protein > genome>template. Figure 6.c indicates that permutation entropy for template species is greater than genome species. On the basis of Figure.6.c permutation entropy for genome species is bigger than structural protein in intracellular viral model which may be doubtable prediction. According to Figures 2.a,b and Figure 3 dynamical trajectory for the population of template is unpredicted than the other two species namely genome and structural proteins species. The trend of permutation entropy is not flat for three species namely structural protein, genome, and template. More permutation entropy shows that fluctuation population of template as a function of time is more than genome and structural species. On the basis of Figure 2 stochastic result of genome species shows that population of genome does not have significant fluctuation population as a function of time. As a result, permutation entropy is not able to give correct result regarding the complexity of stochastic dynamics of intracellular viral reaction.

3.3. Multi Scaling Entropy

3.3.1. Multi scaling entropy with including constant standard deviation of population

3.3.1.a. Multi scaling entropy for genome

Multi scaling entropy calculation is extended for comparison the ability for prediction the complexity for population dynamics of three species in intracellular viral reaction kinetics. The stochastic dynamics for population number versus time is used for computation of multiscaling entropy. We make coarse graining of population number of each species from simulation data. Multiscaling entropy is calculated basis on reference [4,5,12].

Let $\{X_i\} = \{x_1, x_2, \dots, x_N\}$ represent a time series of population each species of length N in stochastic dynamics of intracellular reaction kinetics. Consider the m -length vectors: $u_m(i) = \{x_i, x_{i+1}, \dots, x_{i+m-1}\}$. Following definition for the distance between two vectors in intracellular reaction dynamics

$d[u_m(i), u_m(j)] = \max[|x(i+k) - x(j+k)| : 0 \leq k \leq m-1]$ Let $n_{i,m}(r)$ represent the number of vectors $u_m(j)$ within r of $u_m(i)$. Therefore; $C_i^m(r) = \frac{n_{i,m}(r)}{N-m+1}$ represents

the probability that any vector $u_m(j)$ is within r of $u_m(i)$. Following equation

$$\phi^m(r) = \frac{1}{(N-m+1)} \sum_{i=1}^{N-m+1} \ln C_i^m(r) \quad (15)$$

could be used for calculation multiscaling entropy. For calculation of multiscaling entropy, we calculated standard deviation(SD) our initial simulation data then, we compute number of data which set in distance $r = 0.15SD$. The result of multiscaling entropy as a function of scaling factor for low to high infection level for genome species is shown in Figure 7.a. According to the Figure.7.a multi scaling entropy value increases with increase template population in range number 1-5 and after 5 templates as a initial population, multi scaling decreases with template significantly. On the basis of Figure.7.a multi scaling entropy increases with scale factor linearly.

3.3.1.b. Multi scaling entropy for structural protein

Multi scaling entropy calculation has been extended for structural protein versus scaling factor. Multi scaling entropy result for structural protein shows that there is linear relationship versus scaling factor for initial population of template species at range 1-8.

One peak in multi scaling entropy as a function of scaling factor for structural protein species could be observed for initial template species at population range

$9 \leq \text{Temp} \leq 10$. Result of multiscaling entropy for structural protein species at initial template population 2, 3 and 10 numbers are presented at Figure.7.b and Figure7.c respectively.

3.3.1.c. Multi scaling entropy for Template

Multi scaling entropy has been calculated for low, medium and high infection level of template species versus scaling factor. For low, medium, and high infection level multi scaling entropy trend is completely different to each other. Result of multi scaling entropy versus scaling factor for low, medium and high infection level for dynamical template species has been presented at Figure 8.a, b, c respectively. On the basis of Figure.8.a in low infection level multiscaling entropy increases with scale factor linearly. According to the Figure.8.a multiscale entropy for template species increases versus scale factor in low infection level. In medium infection level, there is non monotonic behavior for multiscaling entropy versus scaling factor for template species. Result of mutiscaling entropy as a function of scaling factor for initial template population, $\text{Temp}=4$, has been presented at Figure.8.b. Multiscaling entropy trend in high infection level for stochastic dynamics in intracellular reaction is reversed in comparison with low infection level completely. For high infection level multiscaling entropy decrease with the scaling factor and there is crossover for multiscaling entropy versus scaling factor with the different initial population of template. Result of multiscaling entropy as a function of scaling factor in high infection level is presented at Figure.8.c.

Comparison of multiscaling entropy versus scaling factor for intermediate infection level for template, structural protein and genome species has been done and its result has been presented at Figure.8.d. On the basis of Figure.8.d there is a following order for multi scaling entropy: template > structural protein > genome.

3.3.2. Scaling entropy with including variation standard deviation of population

For computation of multiscaling entropy in part 3.3.1 standard deviation was constant and r parameter was set $r = 0.15SD$. As a matter of fact for each scaling factor in during of coarse graining method, standard deviation is not constant.[12] Multiscaling entropy based on variation of standard deviation (modified multi scaling entropy) from Gillespie algorithm for stochastic dynamics is calculated for each scaling factor parameter. For each scaling factor standard deviation is calculated; therefore, r is set as $0.15SD$. As a result, modified multiscaling entropy is calculated as a function of scaling factor.

Computation result of modified multiscaling entropy for genome species for each scaling factor is shown in Figure 9.a. On the basis of Figure.9.a modified multiscaling entropy changes with scaling factor linearly for all initial template population. Modified multiscaling entropy value increases versus scaling factor for low-medium infection level and for high infection level, multiscaling entropy decreases again.

Modified multiscaling entropy of structural protein shows that modified multiscaling entropy increases with scaling factor linearly for initial template population $1 \leq \text{Temp} \leq 8$. Result of modified multi scaling entropy for structural protein with initial condition $\text{Temp}=1$ has been presented at Figure.9.b. When number of initial template species increases to 10, then one maximum peak observed in modified multiscaling entropy versus scaling factor for structural protein species.

Modified multi scaling entropy calculation has been extended for template species for different initial population of template species and its result is presented at Figure.9.d. On the basis of Figure.9.d modified multi scaling entropy decreases with scaling factor monotonically. It is worthwhile to notice that there is no regular trend for multi scaling entropy versus scaling factor for template species; however modified multiscaling entropy of template has a regular trend for different initial number of template species. Comparison of modified multiscaling entropy versus scaling factor has been done for three kinds of species, namely genome, structural protein and template. Result of comparison for modified multiscaling entropy has been shown in Figure.9.e. On the basis of Figure.9.e there is a following order for modified multiscaling entropy
Template > Structural Protein > genome.

3.3.3. Initial Template effect on permutation entropy, multiscaling entropy and modified multiscaling entropy

Permutation entropy for three kind of species namely genome, structural protein, template has been calculated for different initial template population. On the basis of permutation entropy result, there is monotonic behavior for permutation entropy value versus initial population of template species in all time. Calculation of multiscaling entropy has been extended as a function of initial template species. Multiscaling entropy shows that there is a non-monotonic behavior for entropy versus initial template population for all species namely gen, structural protein and template. Generally modified multiscaling entropy is monotonic versus scaling factor for genome, structural protein and template species. Result of permutation entropy, multiscaling entropy and modified multiscaling entropy versus initial population of template for template species is

presented at Figure.10.a, b, c respectively. On the basis of Fig.10 for template species there is non monotonic behavior for both multiscaling entropy and modified multiscaling entropy versus initial template population.

4. Conclusion

Kinetics Monte Carlo simulation has been done for intracellular viral reaction kinetics. Gillespie algorithm is used for investigation the population dynamics of three species structural proteins, template, and genome. Reaction equilibrium time is obtained as a function of initial population template species. On the basis of kinetics Monte Carlo result, there is power law as a $f_{eq\ time}(N) = aN^b$ between reaction equilibrium time and initial population of template species. Kinetics Monte Carlo simulation shows that reaction equilibrium time decreases with initial number of template species. Permutation entropy is calculated for three species of viral reaction kinetics. Permutation entropy result depends on windows in low permutation order, however in high permutation order $n \geq 6$ the permutation entropy value is not depend on the windows value. Two clear peaks for permutation entropy of structural protein can be observed in low infection level however in high infection level one peak is observed versus time (day). In addition to multiscaling entropy is calculated on the basis of constant and variation standard deviation for each scale factor. Multiscaling entropy and modified multiscaling entropy have same prediction regarding the magnitude of entropy value and they show the following order: template > structural protein > genome. It is worthwhile to notice that the result of trend for multiscaling entropy of template versus scaling factor depends on initial template population. There is three different behaviors for multiscaling entropy for

template species versus scaling factor. In low infection level multiscale entropy for template species increases with scaling factor monotonically however in Temp=4 as a initial population there is minimum in multiscale entropy for template specie. In high infection level multiscale entropy for template species decreases versus scaling factor monotonically. For genome species, multiscale entropy versus scaling factor shows monotonic behavior. Modified multiscale entropy for template species decreases with scaling factor for all initial template population monotonically. For structural protein multiscale entropy and modified multiscale entropy in low and medium infection level versus scaling factor is monotonic however in very high infection level there is a peak for both multi and modified multiscale entropy as a function of scaling factor. Permutation entropy in presence and absence of chaotic noise is not able to predict complexity for dynamical population of intracellular viral reaction kinetics however multiscale and modified multiscale entropy able to predict the natural complexity for dynamical population of intracellular viral reaction kinetics.

Conflict of Interest: The author declare that he has no conflict of interest.

References:

- [1] Allen, L. J. S. Persistence and extinction in Lotka-Volterra reaction-diffusion equations *Mathematical Biosciences*, 65, 1-12. (1983)
- [2] Bandt, C.; Pompe B. Permutation entropy: a natural complexity measure for time series *Physical review letters*, 88 174102(2002)
- [3] Cao, Y.; Tung, W.-w.; Gao, J.; Protopopescu, V.A.; Hively, L.M Detecting dynamical changes in time series using the permutation entropy *Physical Review E*, 70 046217(2004)
- [4] Costa, M.; Goldberger, A L.; Peng C K. Multiscale entropy analysis of complex

physiologic time series *Physical review letters*, 89, 068102(2002)

[5] Costa, M.; Goldberger, AL.; Peng, CK. Multiscale entropy analysis of biological signals *Physical review E*, 71, 021906(2005)

[6]Eckmann, J.-P.; Ruelle, D. Ergodic theory of chaos and strange attractors *Reviews of modern physics*, 57, 617(1985)

[7]Gillespie, D.T. Stochastic simulation of chemical kinetics *Annu. Rev. Phys. Chem.*, 58 , 35-55(2007)

[8] Goldberger, A.L; Peng, C.-K; Lipsitz, L.A. What is physiologic complexity and how does it change with aging and disease? *Neurobiology of aging*, 23, 23-26(2002)

[9] Hayano, J.; Yamasaki, F.; Sakata, S.; Okada, A.; Mukai, S.; Fujinami, T: Spectral characteristics of ventricular response to atrial fibrillation *American Journal of Physiology-Heart and Circulatory Physiology*, 273, H2811-H2816(1997)

[10] Mantas, L., Maosen, C., Minvydas, R. Permutation entropy-based 2D feature extraction for bearing fault diagnosis, *Nonlinear Dynamics*, 102, 1717–1731(2020)

[11] Nichols, J.W.; Flynn, S.W.; Green , J.R. Order and disorder in irreversible decay processes *The Journal of chemical physics*, 142, 064113(2015)

[12] Nikulin, V.V.; Brismar, T. Comment on “Multiscale entropy analysis of complex physiologic time series” *Physical review letters*, 92, 089803(2004)

[13] Pesin, Y.B. Dimension theory in dynamical systems: contemporary views and applications, University of Chicago Press, 2008.

[14]Srivastava, R.; You, L.; Summers, J.; Yin, J. Stochastic vs. deterministic modeling of intracellular viral kinetics , *Journal of Theoretical Biology*, 218, 309-321 (2002)

[15] Taherkhani, F.; Rahmani, M.; Taherkhani, F.; Akbarzadeh, H.; Abroshan, H. Permutation entropy and detrend fluctuation analysis for the natural complexity of cardiac heart interbeat signals *Physica A: Statistical Mechanics and its Applications*, 392 3106-3112 (2013)

[16] Taherkhani, F.; Ranjbar, S *Chemistry: The Key to our Sustainable Future, Stochastic approach for enzyme reaction in nano size via different algorithms 2014 Chapter 14, page 189-206, Springer*

[17] Taherkhani, F.; Taherkhani, F; Rezania, H.; Akbarzadeh, H. Intracellular viral infection kinetics using a stochastic approach *Progress in Reaction Kinetics and Mechanism*, 38, 359-376(2013)

[18] Taherkhani,F.; Taherkhani,F; Permutation, Multiscale and Modified Multiscale Entropies a Natural Complexity for Low-High Infection Level Intracellular Viral Reaction Kinetics

<https://scirate.com/?date=2016-07-26&page=12&range=1>

[19] Xuegeng, M., P. Shang, Albert C. Y , Chung-Kang, P. Multiscale cumulative residual distribution entropy and its applications on heart rate time series, *Nonlinear Dynamics* , 101, 2357–2368(2020)

Figure Captions:

Figure.1. Equilibrium time for template species as a function of initial population of template.

Figure.2. Typical one kinetics Monte Carlo for genome species with two different kinds of algorithms, Gillespie, Poisson. b) Kinetics Monte Carlo simulation for structural protein as a function of time via Gillespie, Poisson algorithm.

Figure.3. Same as Fig.2 one kinetics Monte Carlo simulation run for template with Gillespie and Poisson algorithms.

Figure.4. a) Permutation entropy of genome as a function of time for initial template with number 1, 5,6,10. b) Permutation entropy as a function of time for structural protein at initial template molecule with population 2 and 3. c) Similar to the Figure.4.b permutation entropy for structural protein with the initial population template number 5,6,7,10 d.

d) Permutation entropy of template as a function of time (day) with initial population of template 1,5,10

Figure.5. a) Permutation entropy of genome versus time (day) for different order of permutation entropy $n=2, 4, 6$ for initial template=1. b) Similar to Figure.5.a permutation entropy for different order $n=2, 4, 6$ with initial template=10.

c) Permutation entropy for genome versus time for order $n=4$ but for different windows =512, 1024.

d) Similar to the Figure.5 permutation entropy for genome as a function of time at windows 512, 1024 with $n=6$.

e) Behavior of permutation entropy per symbol $h(n)$ versus n in big time scale of dynamical system.

Figure.6. a) Comparison permutation entropy on the basis of comparison neighborhood value for three species, genome, structural protein, template as a function of time (day) from result of one stochastic trajectory of population with initial template 5.

b) Similar to the Figure.6.a comparison of permutation entropy for three species, genome, structural protein from result of 1000 stochastic population trajectory.

c) Comparison of permutation entropy for genome, structural protein, template with initial template=10 in absence of noise

d) Comparison of permutation entropy for genome, structural protein, template with initial template=10 in presence of noise

Figure.7.a) Multiscaling entropy for genome species versus scaling factor with initial template with number 2, 5,6,10.

b) Multiscaling entropy for structural protein versus scaling factor with initial template 2,3.

c) Multiscaling entropy for structural protein versus scaling factor with initial template 10

Figure.8. a) Multiscaling entropy for template as a function of scaling factor for initial template 1,3.

b) Multiscaling entropy for template versus scaling factor for initial template=4

c) Same as Figure.8.b, Multiscaling entropy for template versus scaling factor for initial template=7,10

d) Comparison of multiscaling entropy for template, genome, structural protein versus scaling factor with initial population of template=3

Figure.9. a) Modified scaling entropy of genome versus scaling factor with different initial template population 1,3,5,6,10

b) Modified scaling entropy of structural protein versus scaling factor with initial template population 1.

c) Same as Figure.9.b modified scaling entropy of structural protein versus scaling factor for initial template=10

d) Modified scaling entropy of template as a function of scaling factor with initial template molecule 1,3,4,5,6,10.

e) Comparison modified multi scaling entropy genome, structural protein, template versus scaling factor with initial template=3.

Figure.10. a) Permutation entropy of template versus initial template population

b) Multiscaling entropy of template versus initial template population

c) Modified multiscaling entropy of template versus initial template population

Figure 1

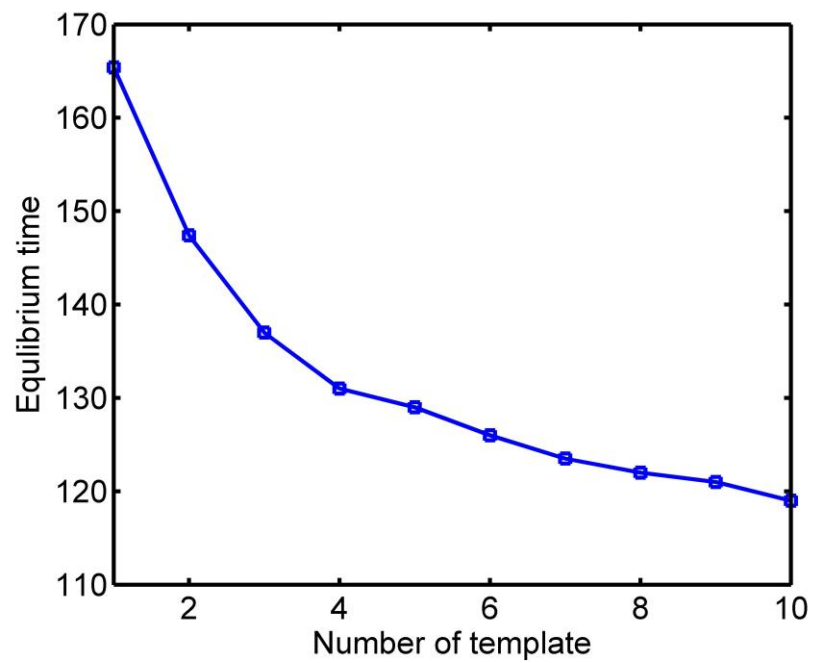


Figure.2.a

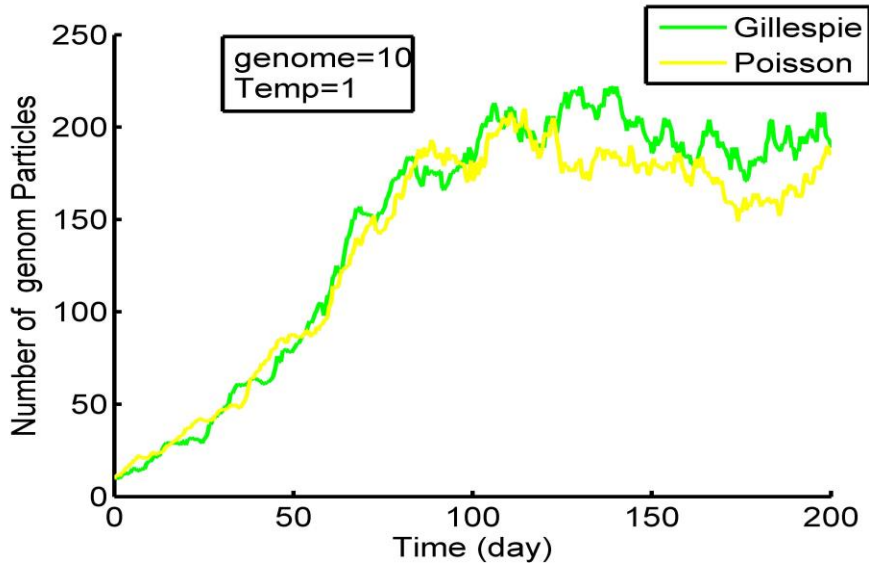


Fig.2.b

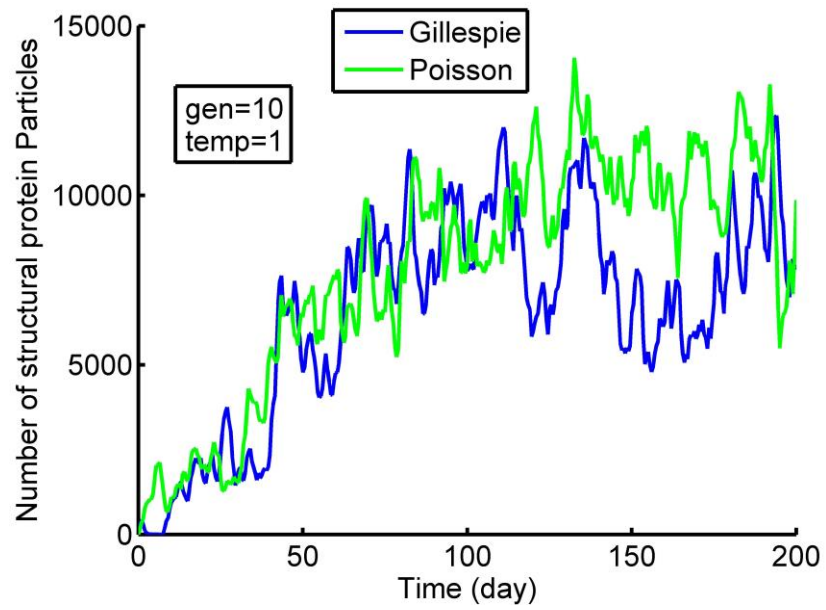
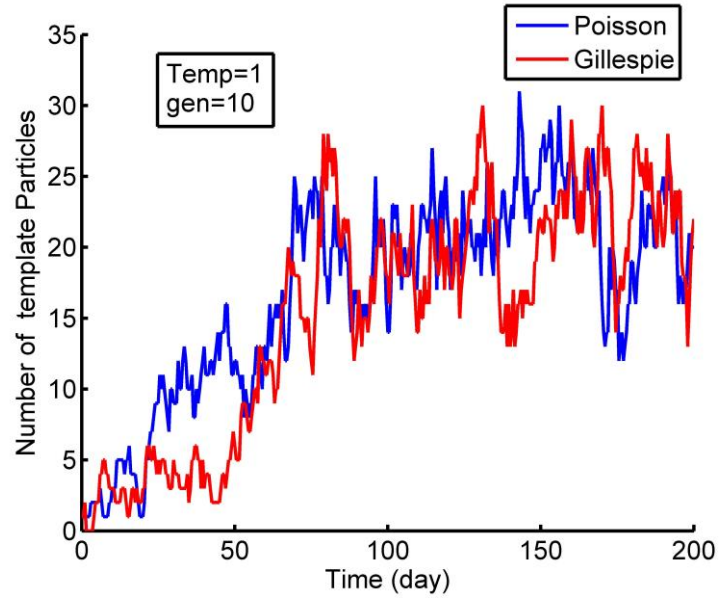


Figure.3.



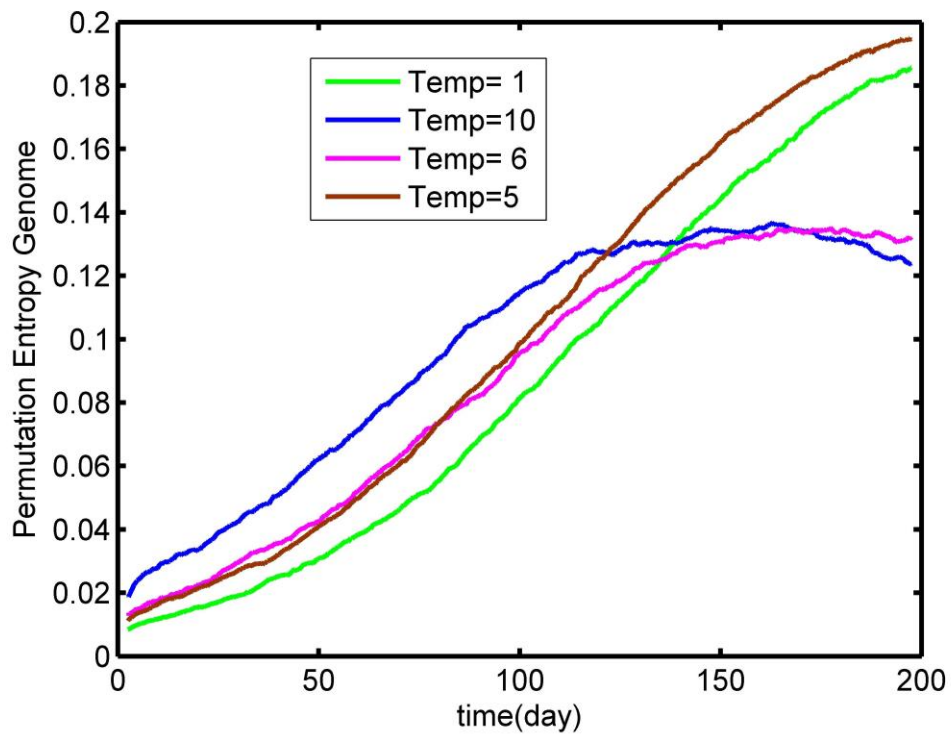


Figure.4.a

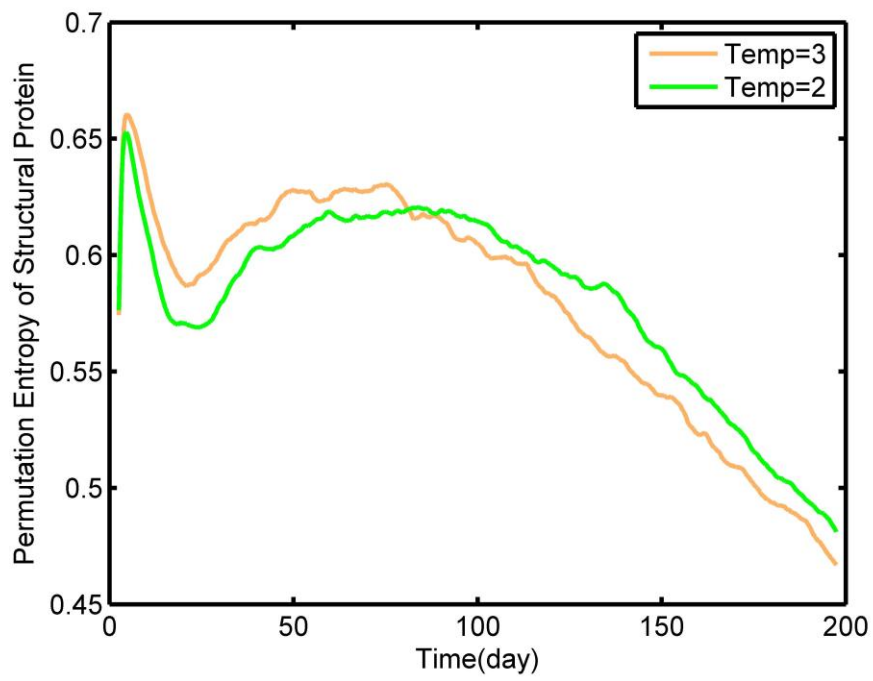


Figure.4.b

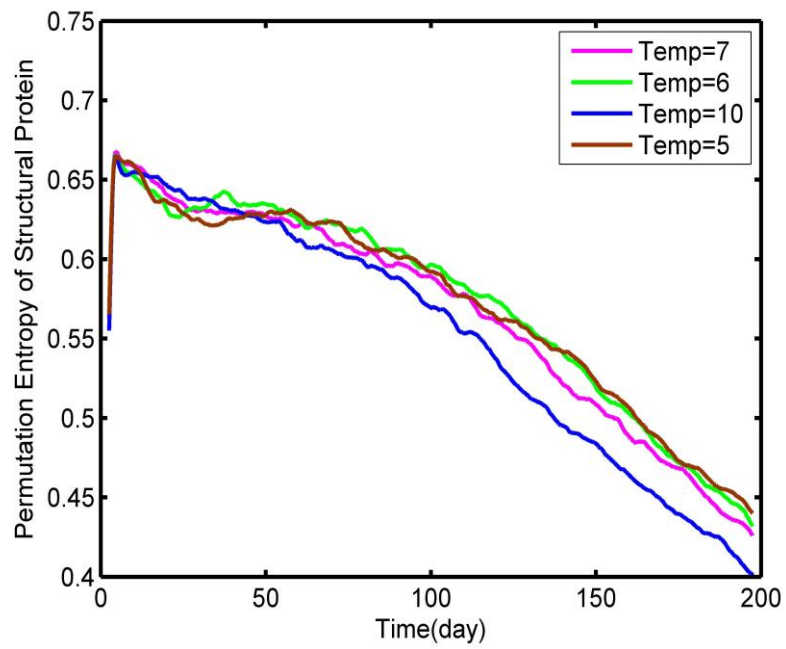


Figure.4.c

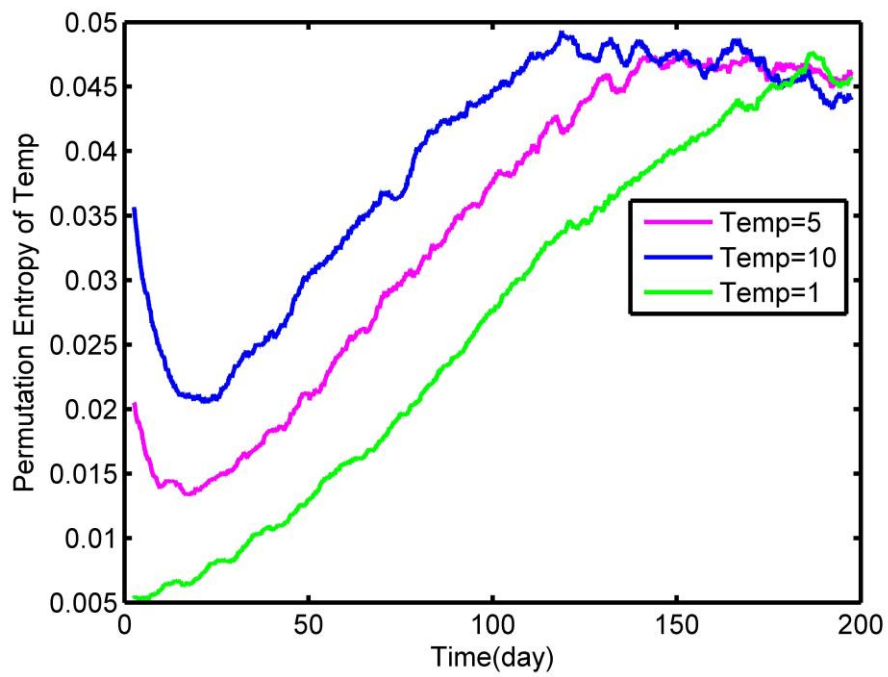


Figure.4.d

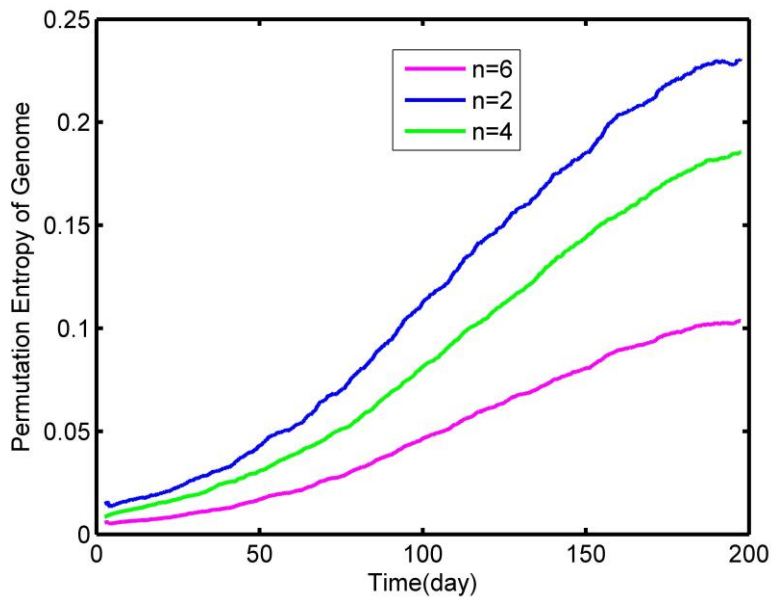


Figure.5.a

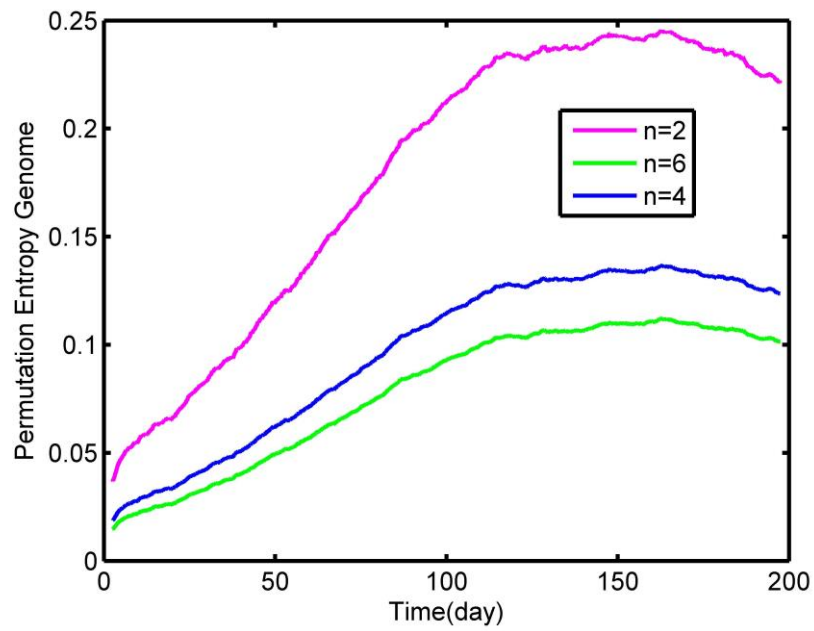


Figure.5.b

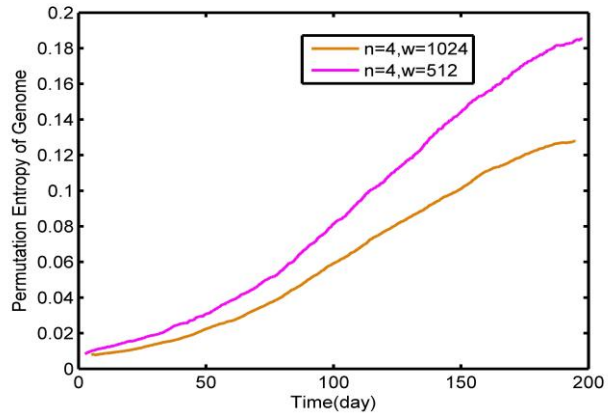


Figure.5.c

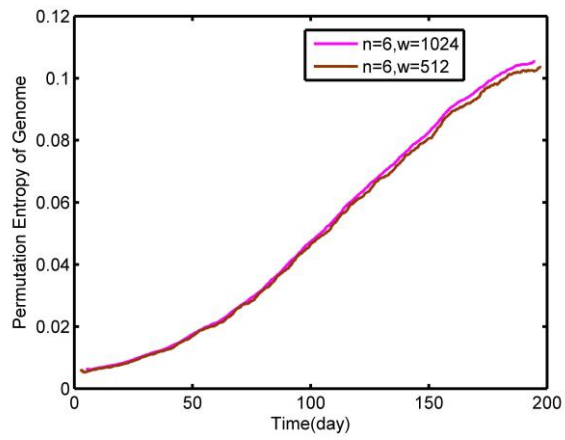


Figure.5.d

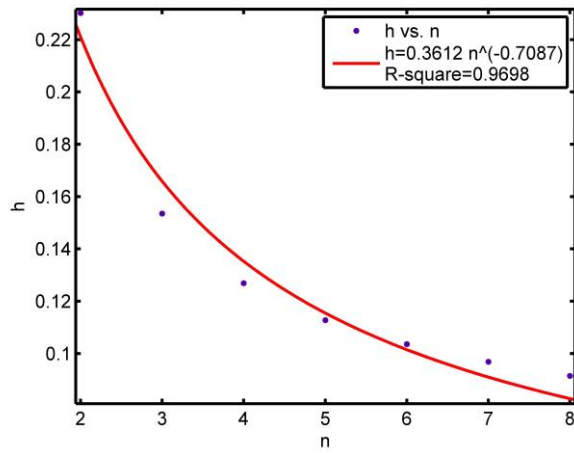


Figure.5.e

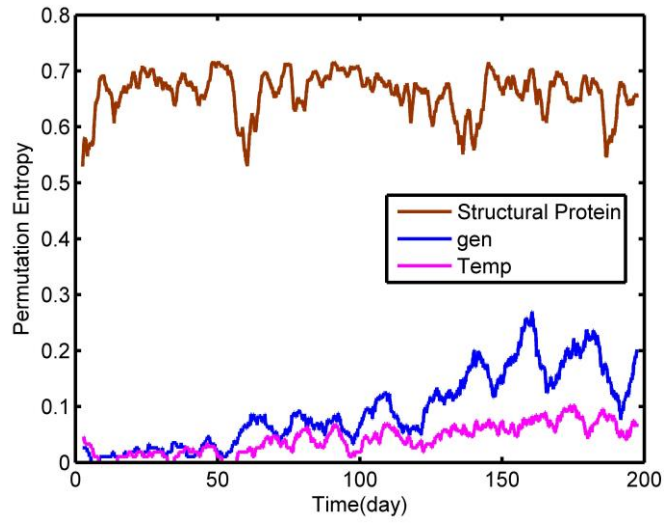


Figure.6.a

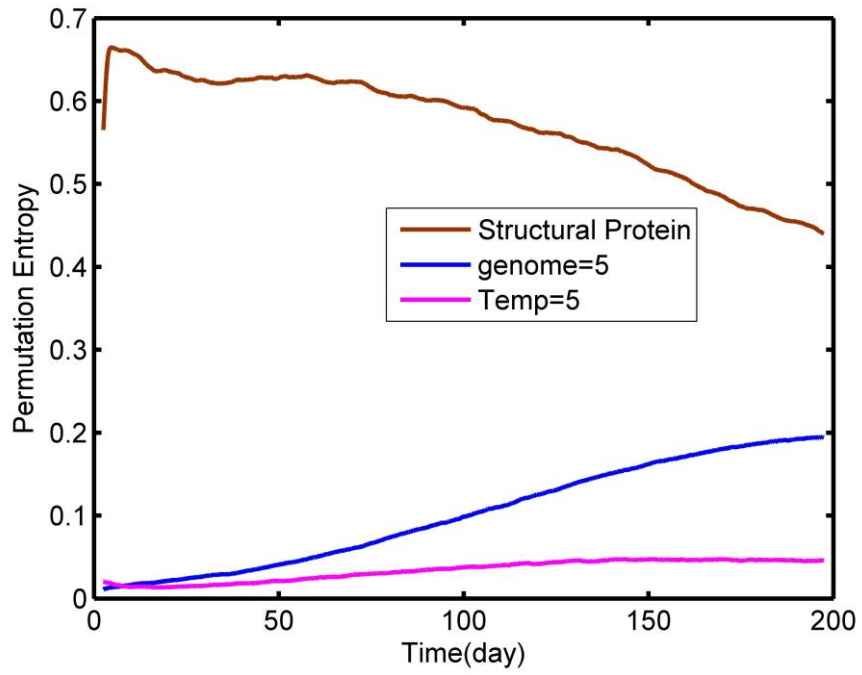


Figure.6.b

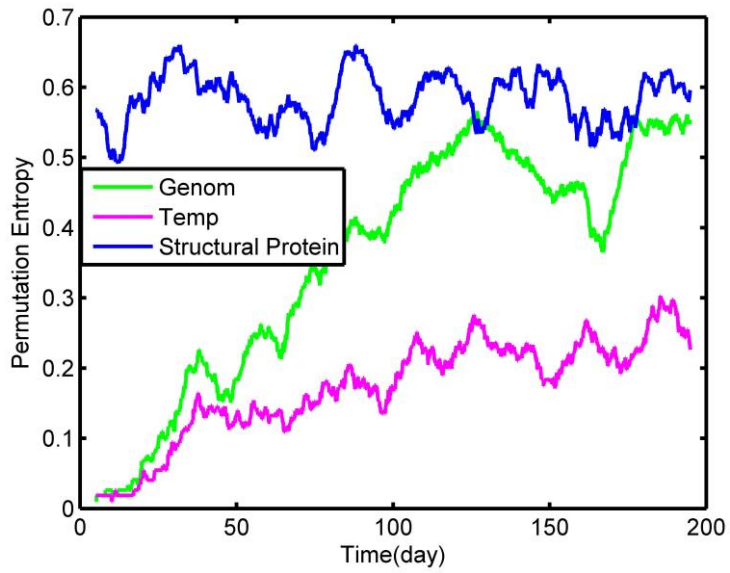


Figure.6.c

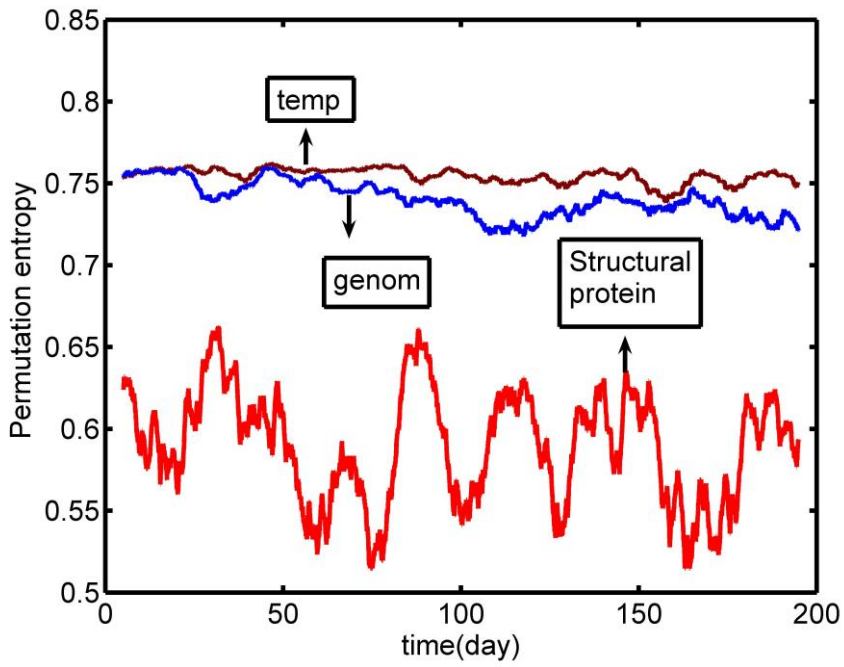


Figure.6.d

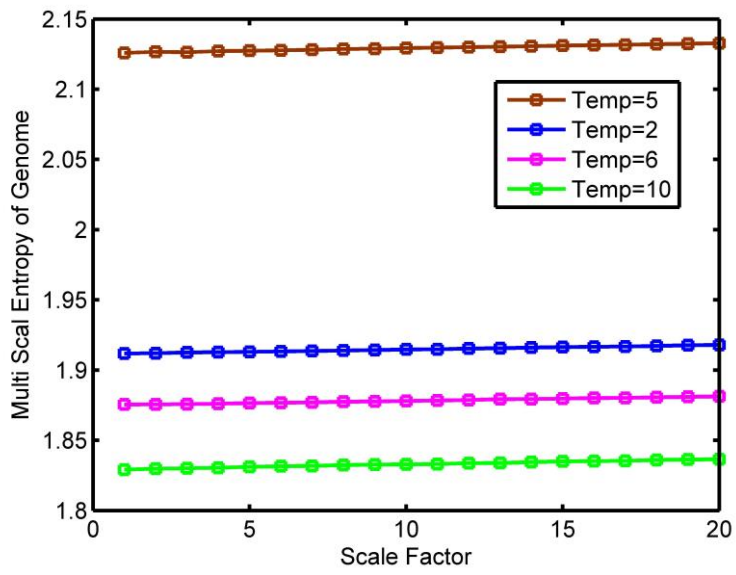


Figure.7.a

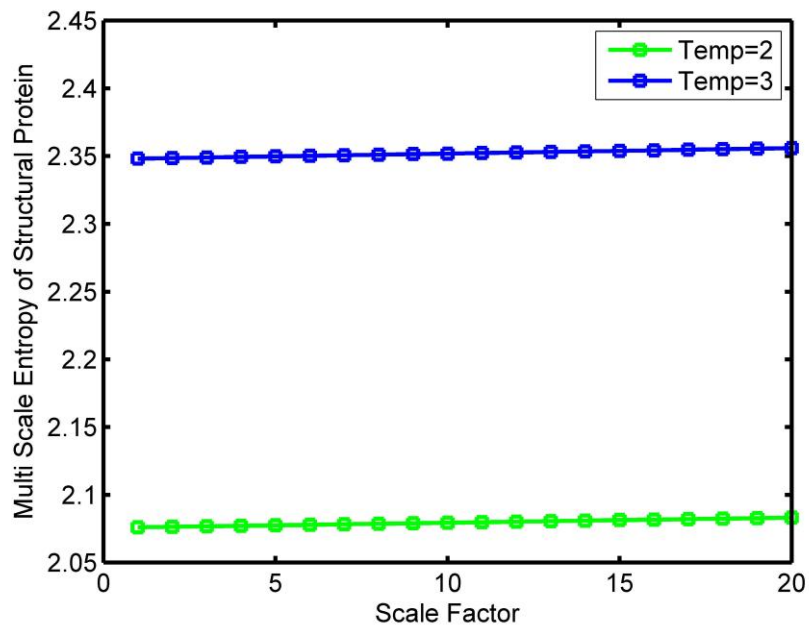


Figure.7.b

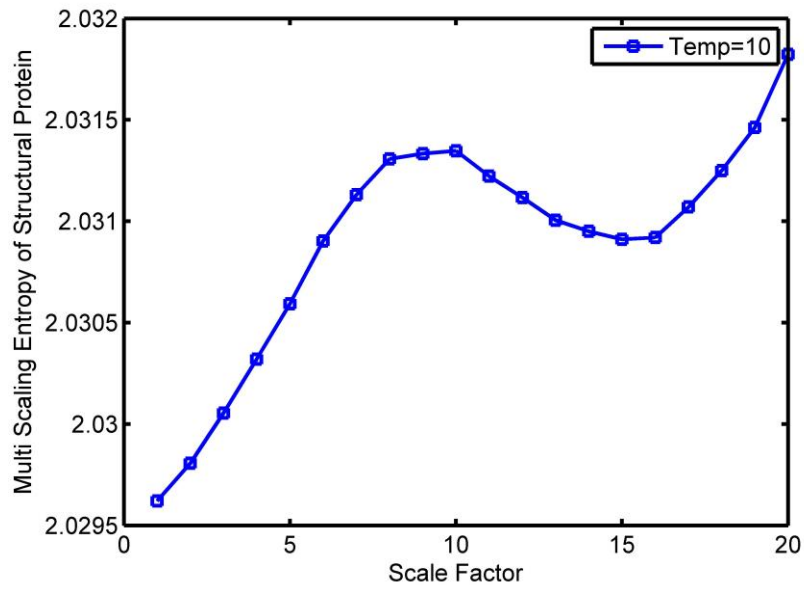


Figure.7.c

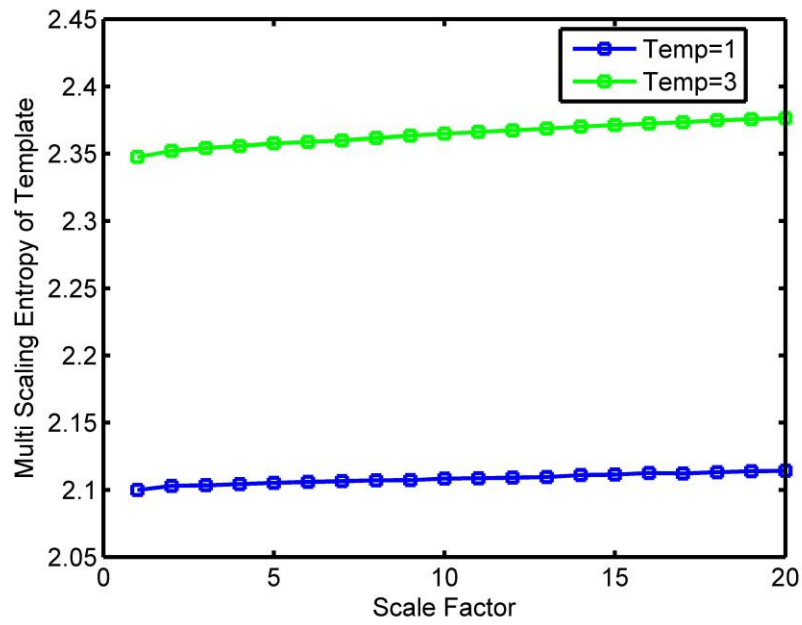


Figure.8.a

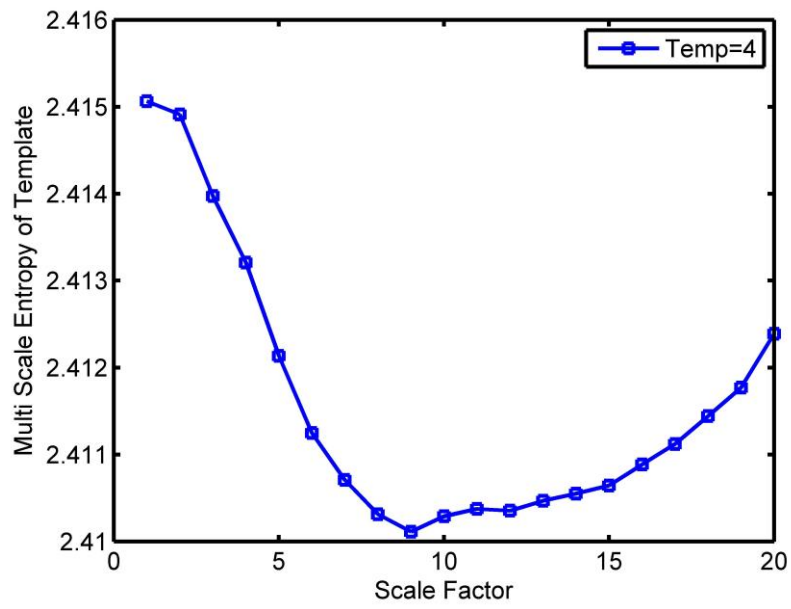


Figure.8.b

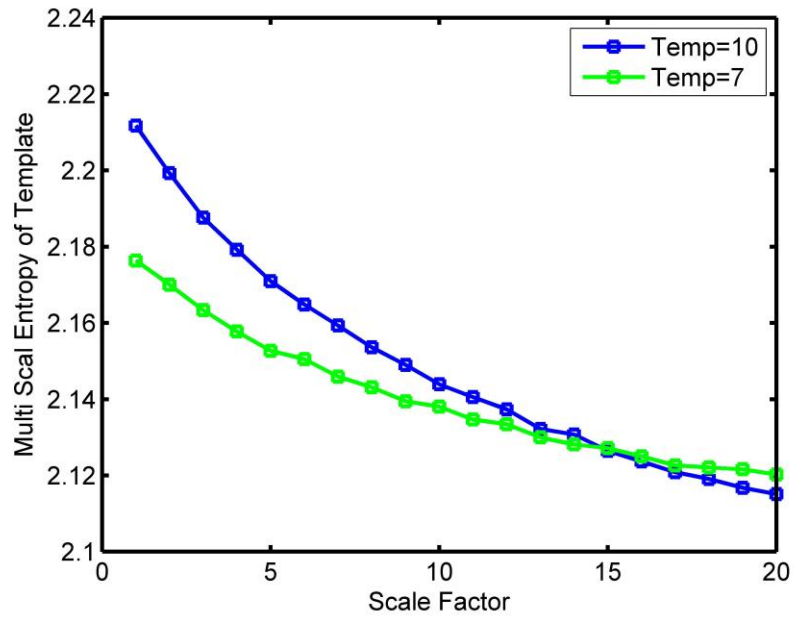


Figure.8.c

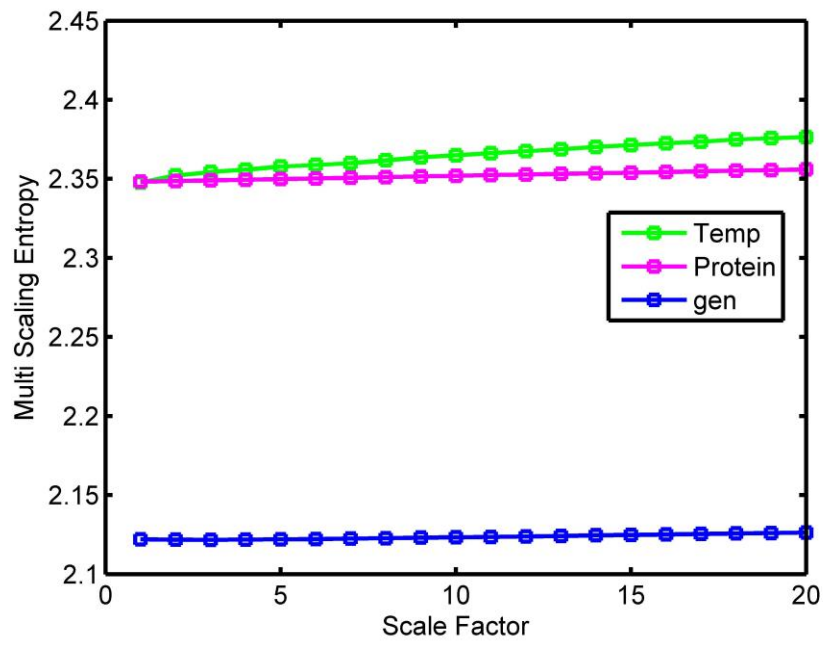


Figure.8.d

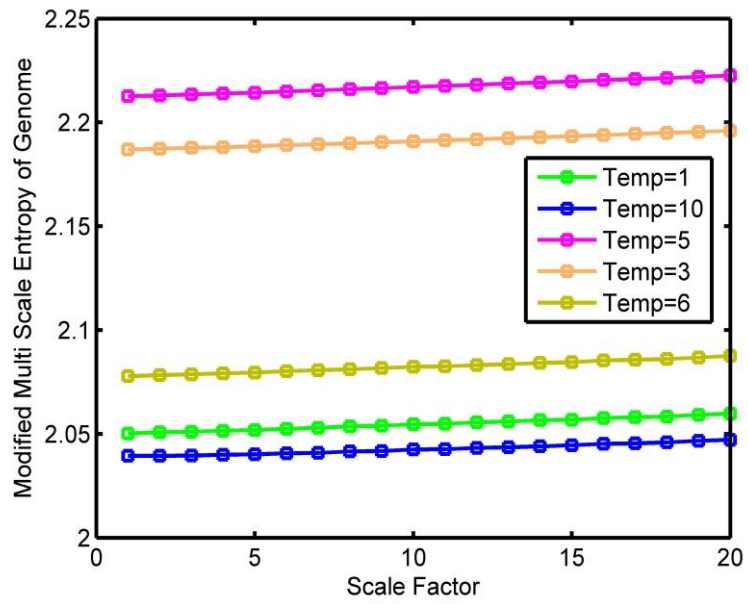


Figure.9.a

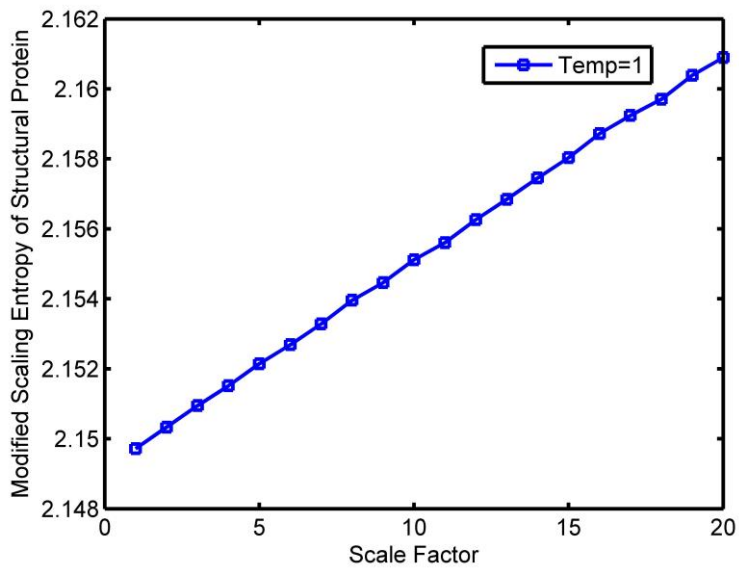


Figure.9.b

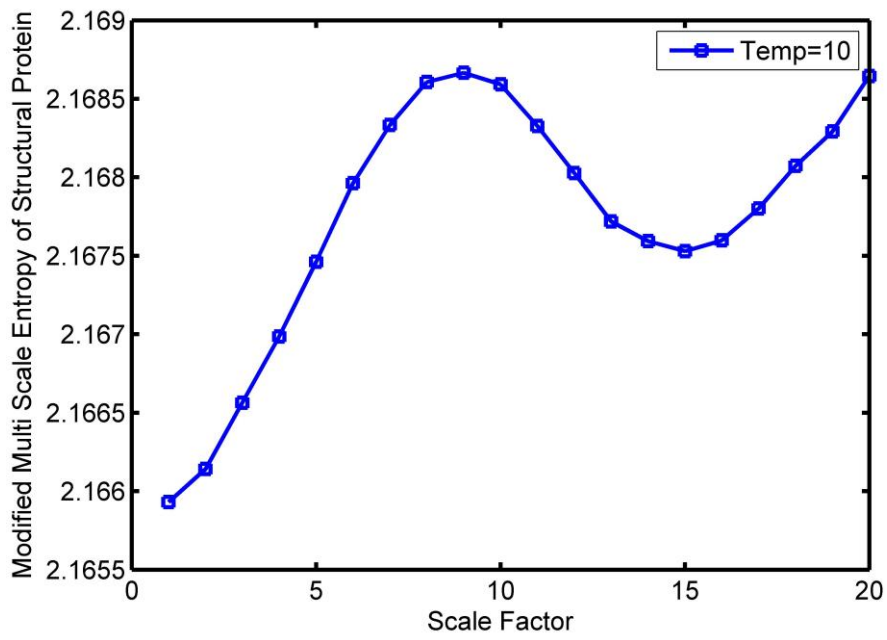


Figure.9.c

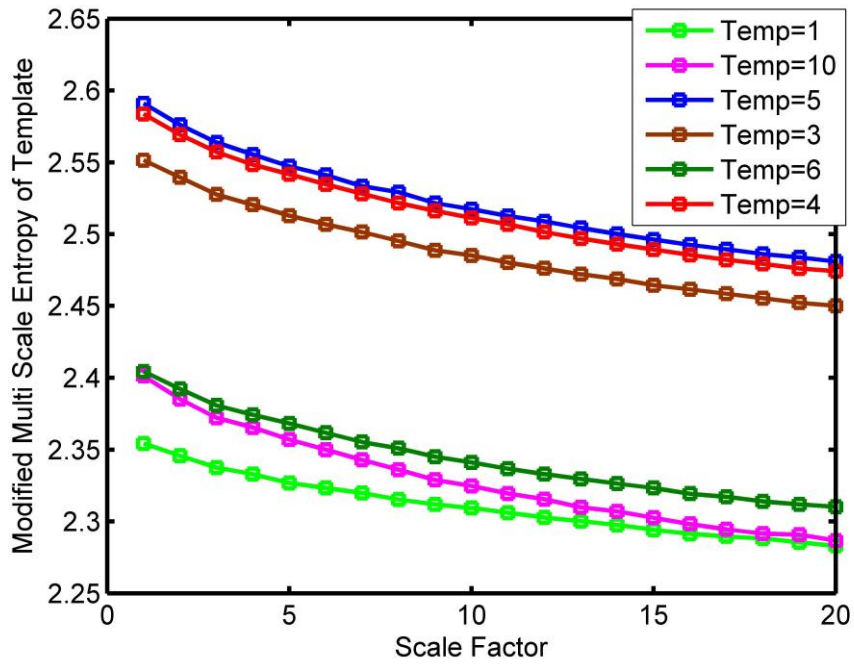


Figure.9.d

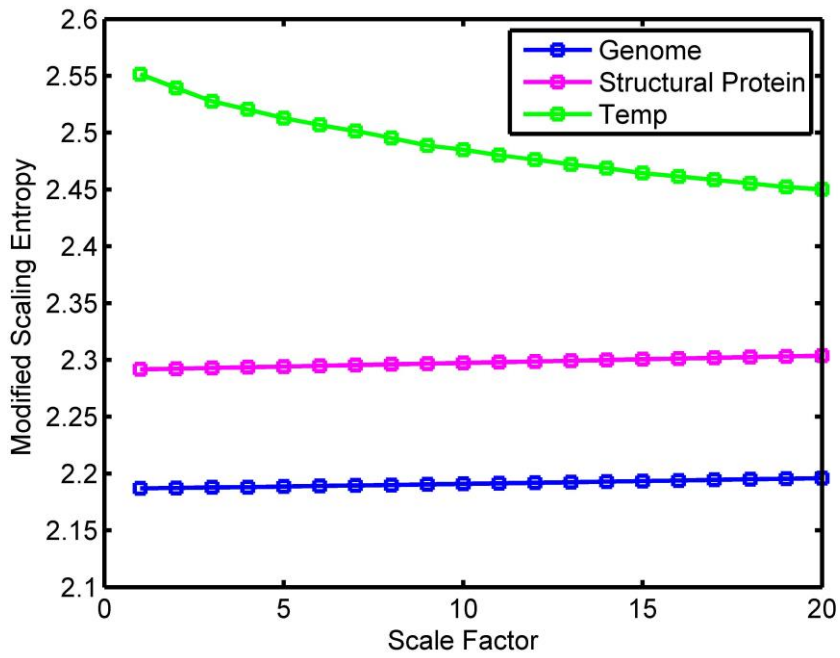


Figure.9.e

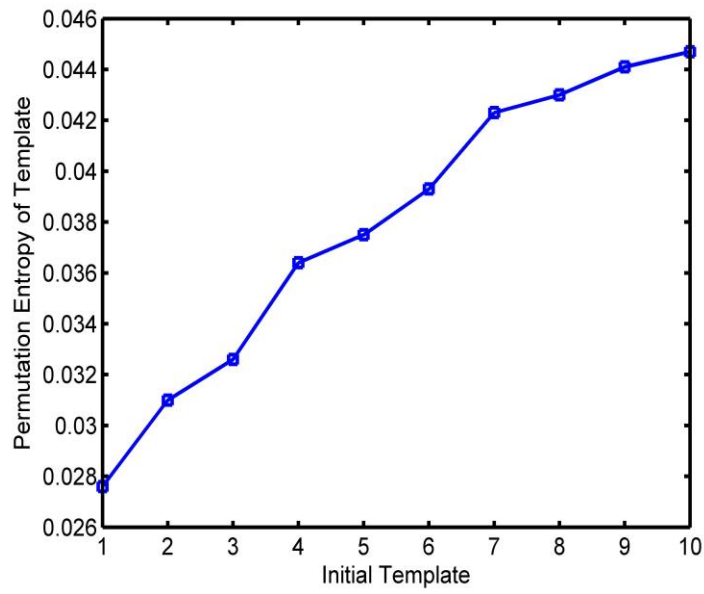


Figure.10.a

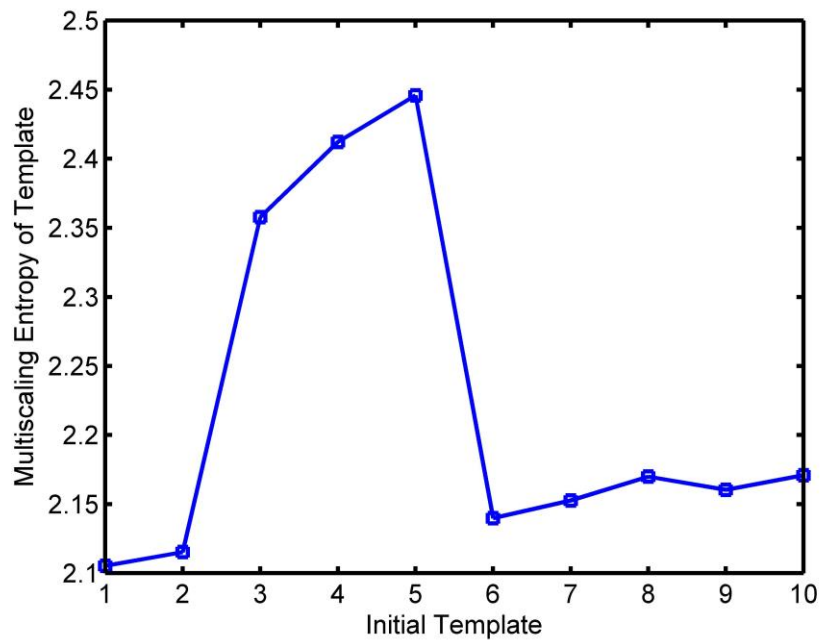


Figure.10.b

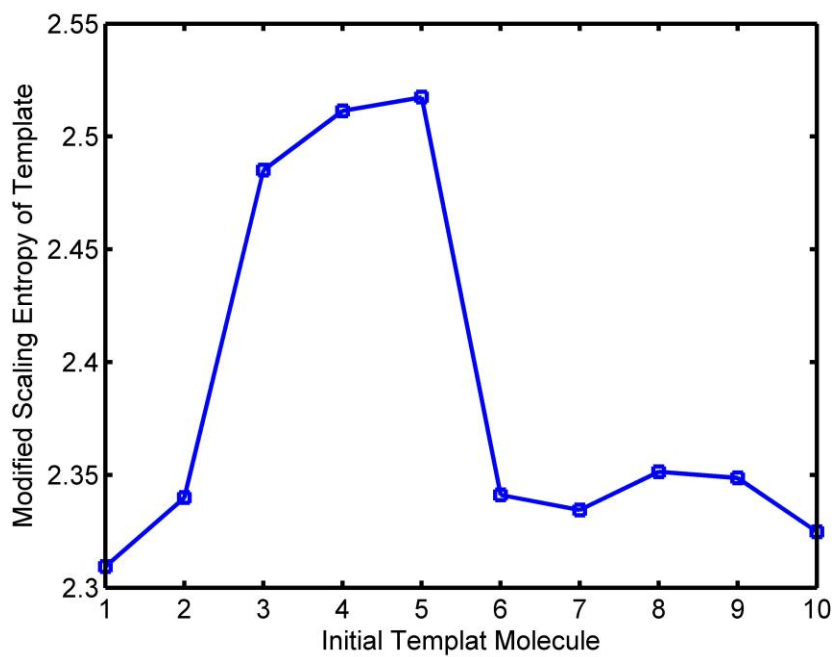


Figure.10.c

Figures

Figure 1

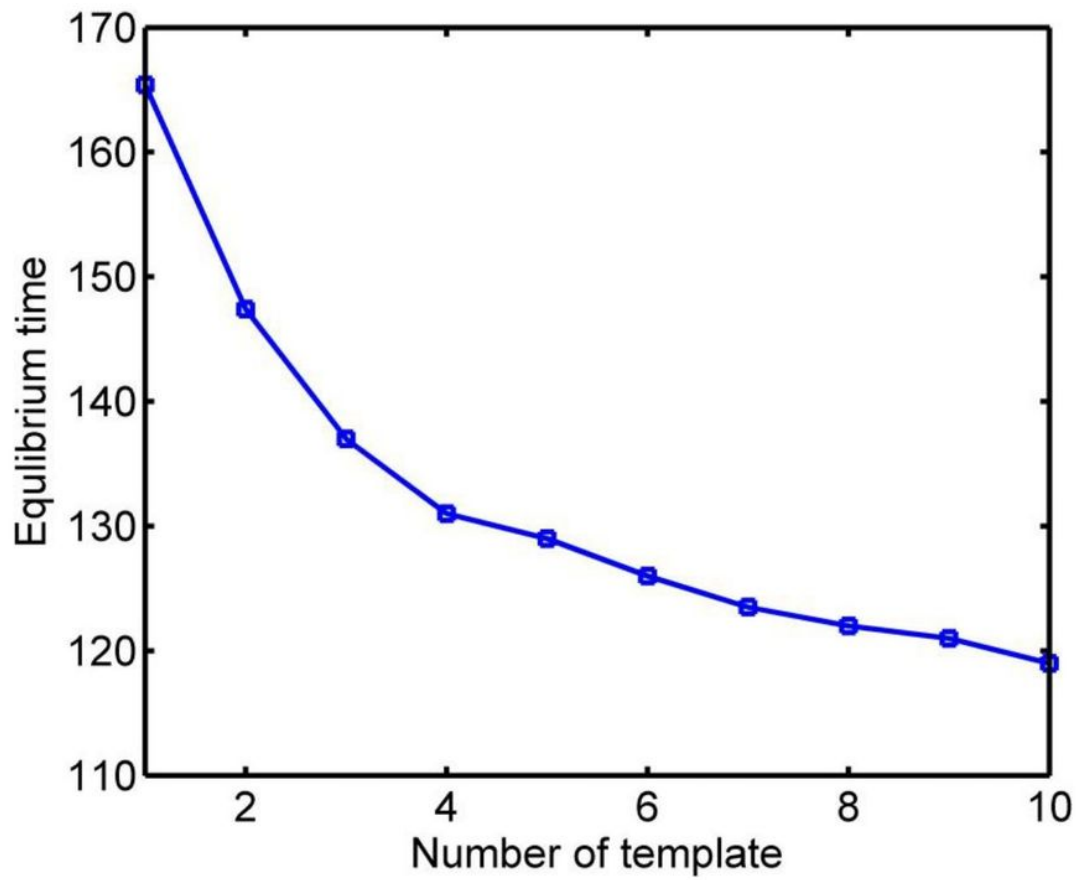


Figure 1

Equilibrium time for template species as a function of initial population of template.

Figure.2.a

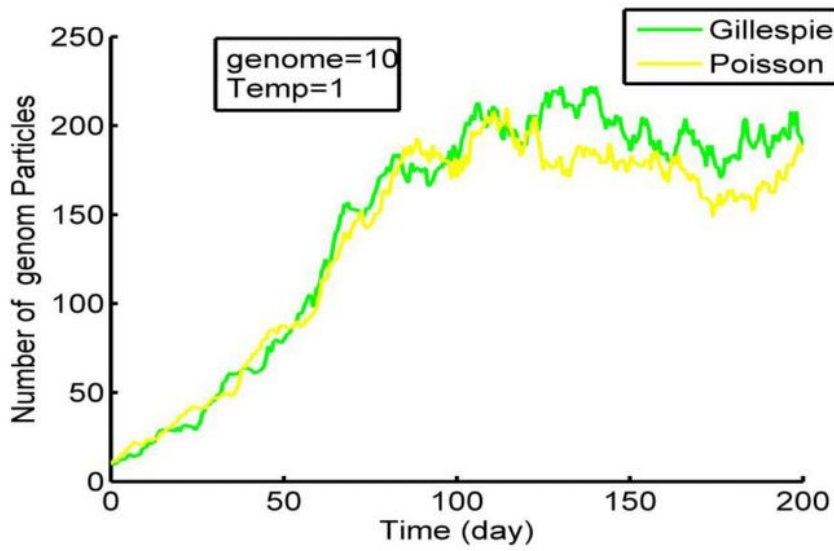


Fig.2.b

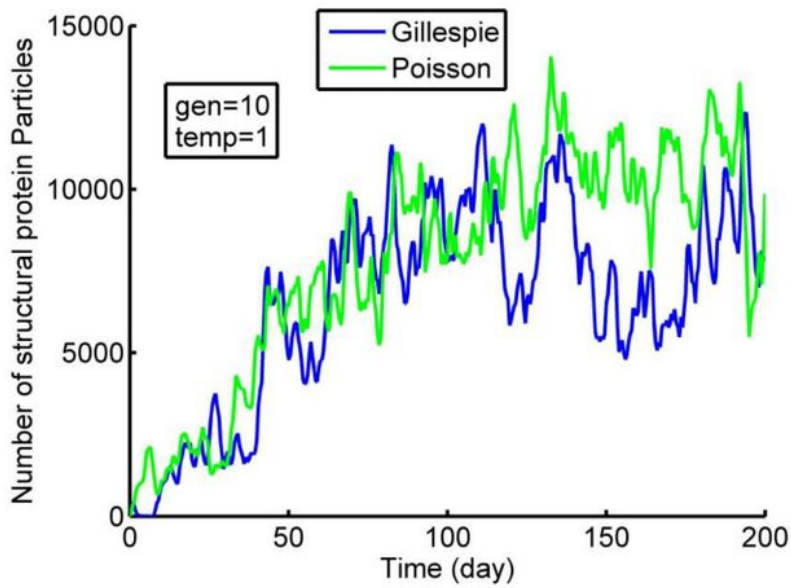


Figure 2

Typical one kinetics Monte Carlo for genome species with two different kinds of algorithms, Gillespie, Poisson. b) Kinetics Monte Carlo simulation for structural protein as a function of time via Gillespie, Poisson algorithm.

Figure.3.

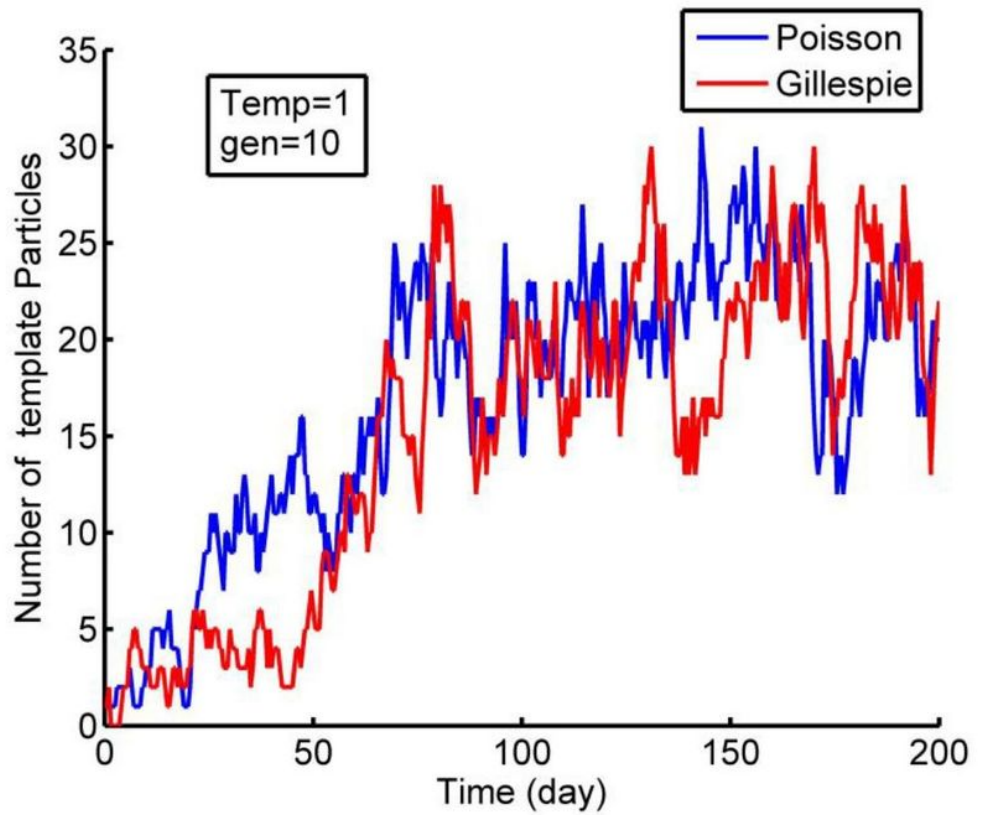


Figure 3

Same as Fig.2 one kinetics Monte Carlo simulation run for template with Gillespie and Poisson algorithms.

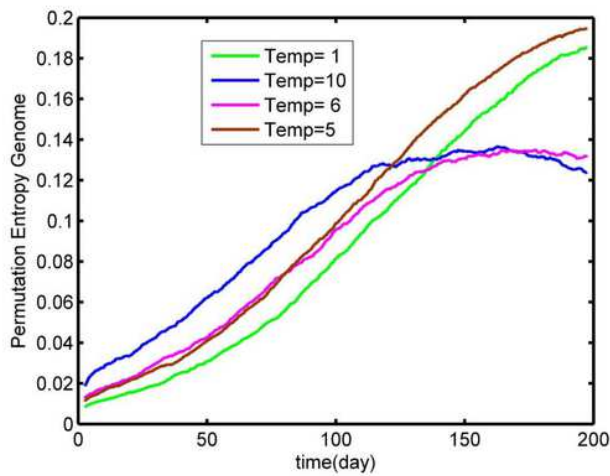


Figure.4.a

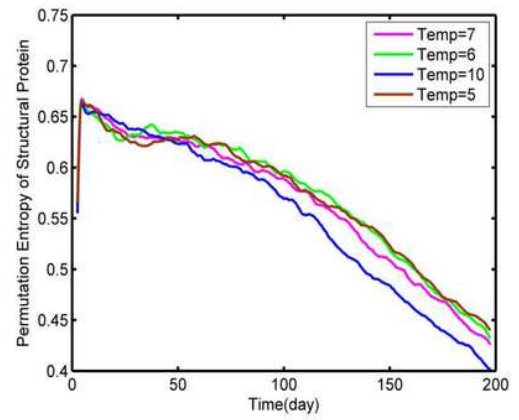


Figure.4.c

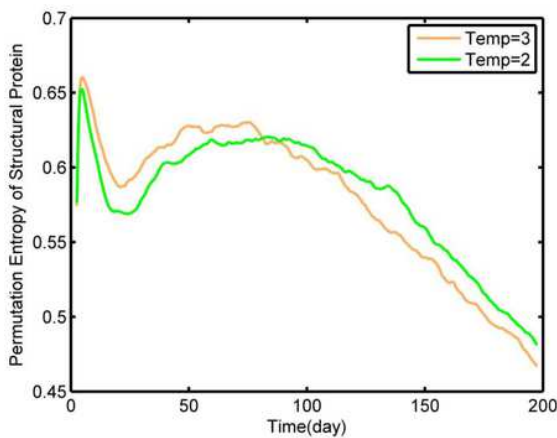


Figure.4.b

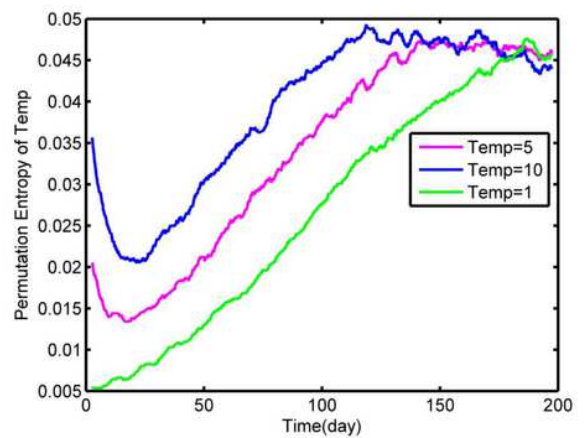


Figure.4.d

Figure 4

a) Permutation entropy of genome as a function of time for initial template with number 1, 5,6,10. b) Permutation entropy as a function of time for structural protein at initial template molecule with population 2 and 3. c) Similar to the Figure.4.b permutation entropy for structural protein with the initial population template number 5,6,7,10 d. d) Permutation entropy of template as a function of time (day) with initial population of template 1,5,10

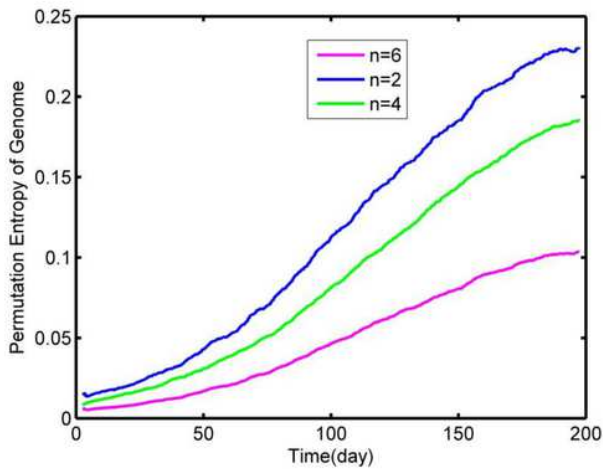


Figure.5.a

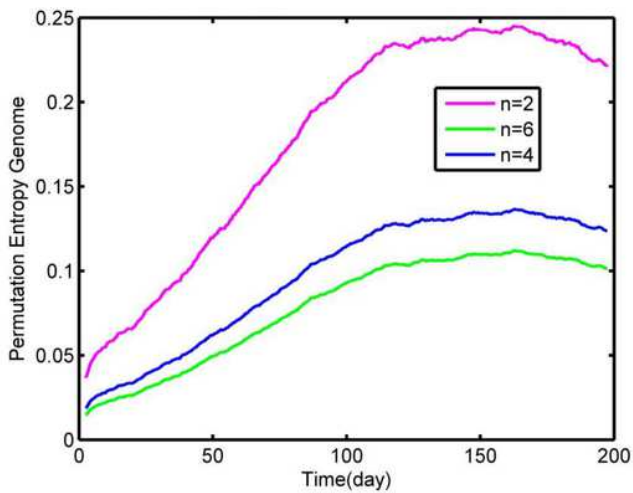


Figure.5.b

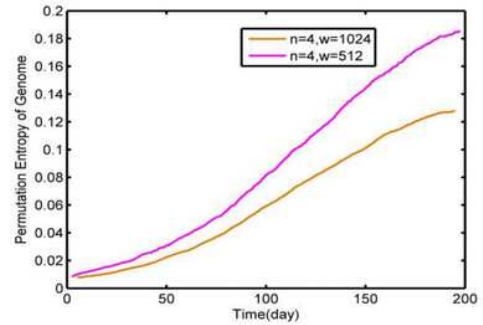


Figure.5.c

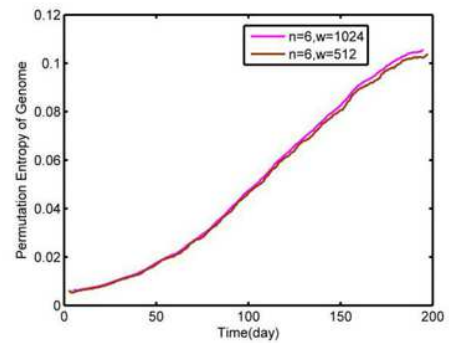


Figure.5.d

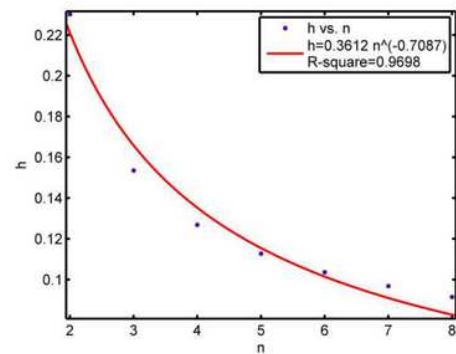


Figure.5.e

Figure 5

a) Permutation entropy of genome versus time (day) for different order of permutation entropy $n=2, 4, 6$ for initial template=1. b) Similar to Figure.5.a permutation entropy for different order $n=2, 4, 6$ with initial template=10. c) Permutation entropy for genome versus time for order $n=4$ but for different windows $w=512, 1024$. d) Similar to the Figure.5 permutation entropy for genome as a function of time at windows 512, 1024 with $n=6$. e) Behavior of permutation entropy per symbol $h(n)$ versus n in big time scale of dynamical system.

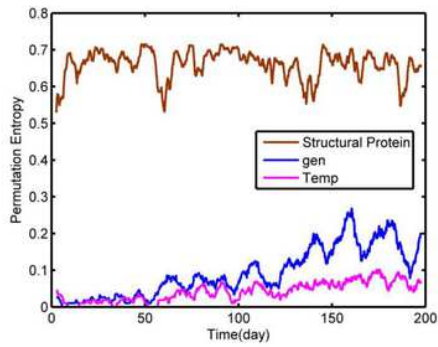


Figure.6.a

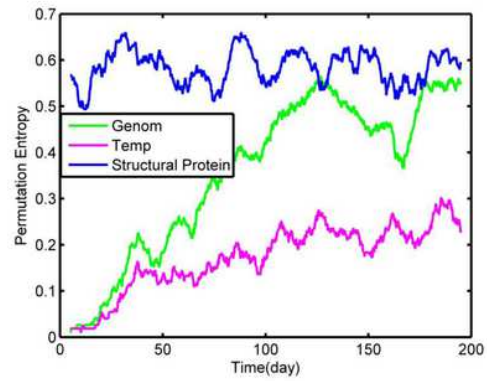


Figure.6.c

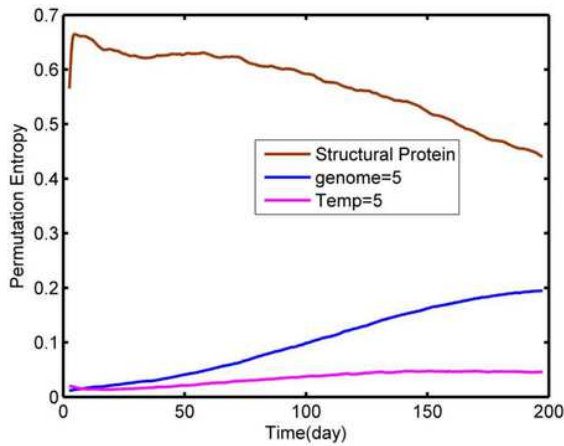


Figure.6.b

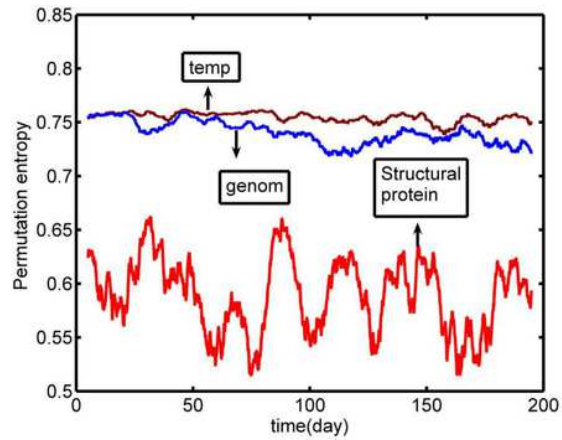


Figure.6.d

Figure 6

a) Comparison permutation entropy on the basis of comparison neighborhood value for three species, genome, structural protein, template as a function of time (day) from result of one stochastic trajectory of population with initial template 5. b) Similar to the Figure.6.a comparison of permutation entropy for three species, genome, structural protein from result of 1000 stochastic population trajectory. c) Comparison of permutation entropy for genome, structural protein, template with initial template=10 in absence of noise d) Comparison of permutation entropy for genome, structural protein, template with initial template=10 in presence of noise

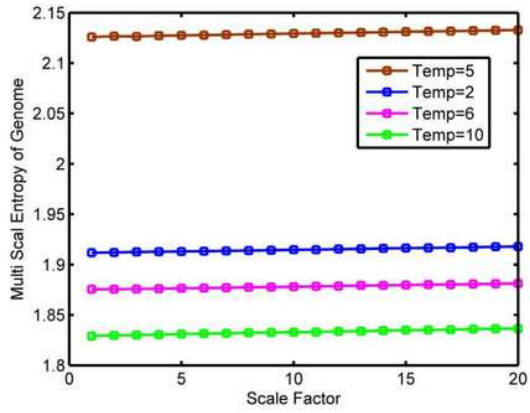


Figure.7.a

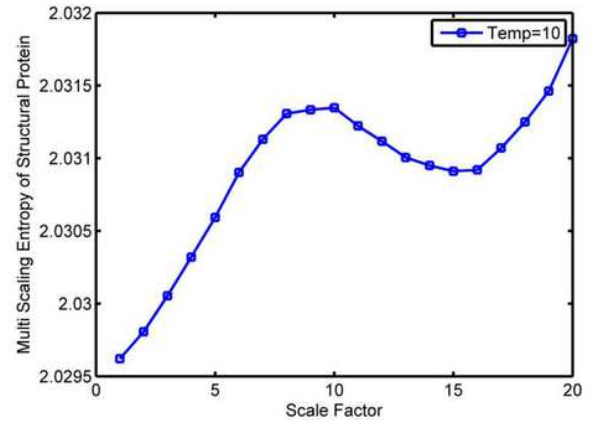


Figure.7.c

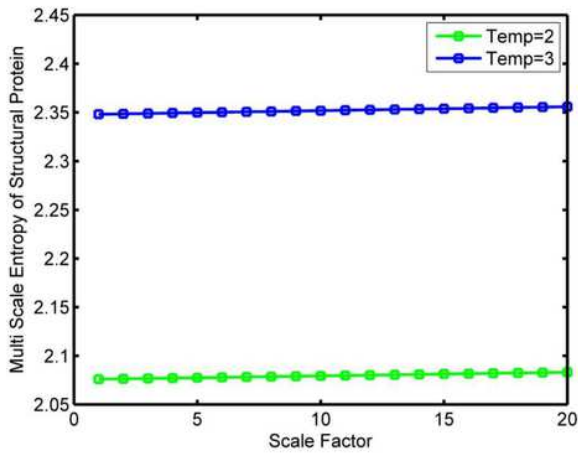


Figure.7.b

Figure 7

a) Multiscaling entropy for genome species versus scaling factor with initial template with number 2, 5,6,10. b) Multiscaling entropy for structural protein versus scaling factor with initial template 2,3. c) Multiscaling entropy for structural protein versus scaling factor with initial template 10

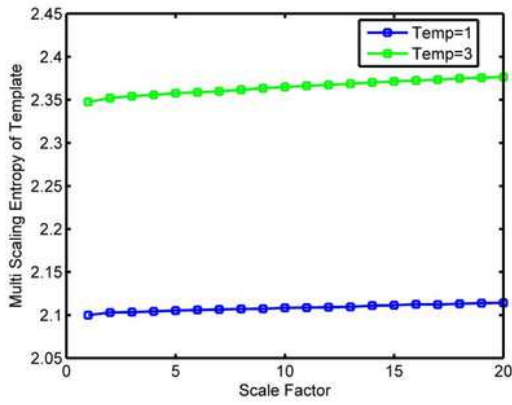


Figure.8.a

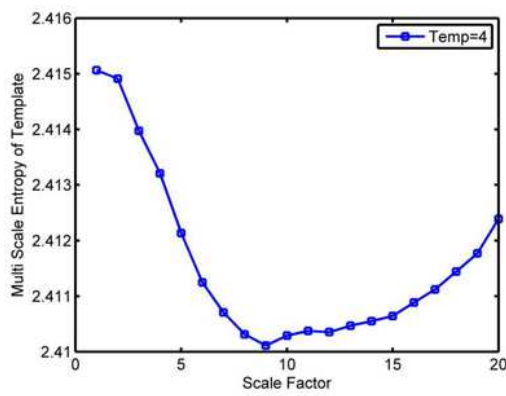


Figure.8.b

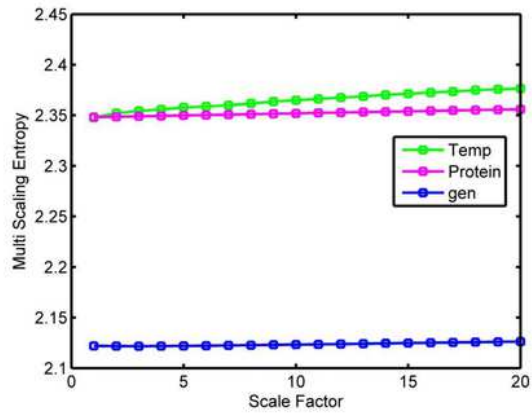


Figure.8.d

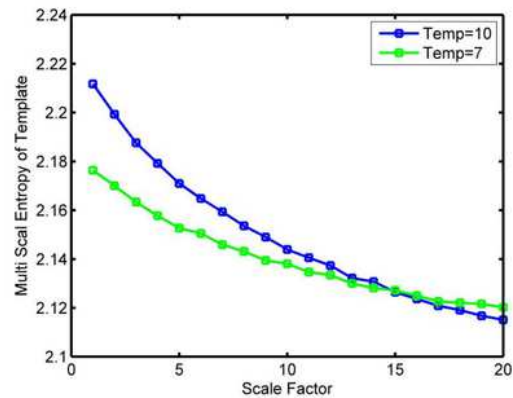


Figure.8.c

Figure 8

a) Multiscaling entropy for template as a function of scaling factor for initial template 1,3. b) Multiscaling entropy for template versus scaling factor for initial template=4 c) Same as Figure.8.b, Multiscaling entropy for template versus scaling factor for initial template=7,10 d) Comparison of multiscaling entropy for template, genome, structural protein versus scaling factor with initial population of template=3

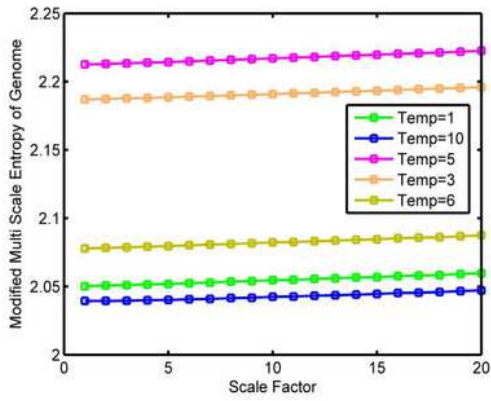


Figure.9.a

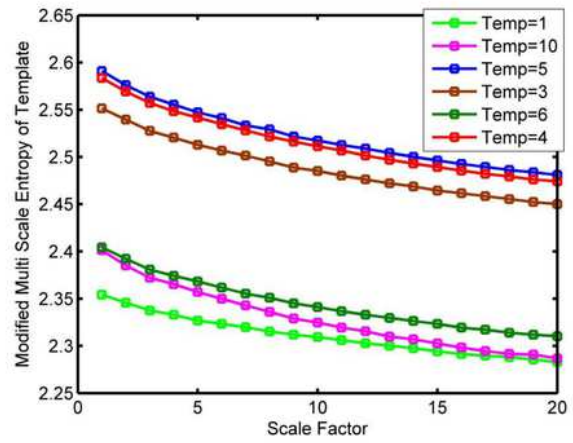


Figure.9.d

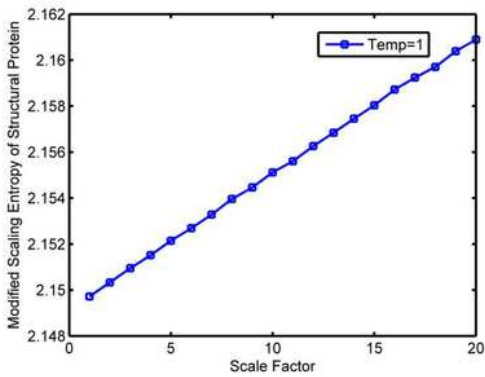


Figure.9.b

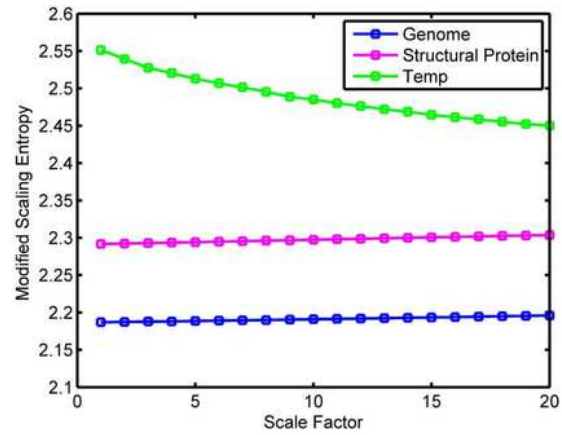


Figure.9.e

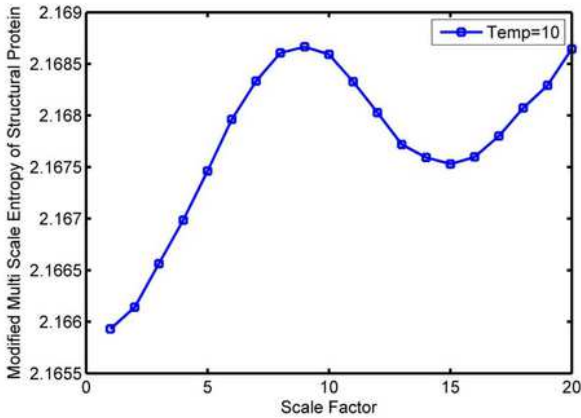


Figure.9.c

Figure 9

a) Modified scaling entropy of genome versus scaling factor with different initial template population 1,3,5,6,10 b) Modified scaling entropy of structural protein versus scaling factor with initial template population 1. c) Same as Figure.9.b modified scaling entropy of structural protein versus scaling factor for initial template=10 d) Modified scaling entropy of template as a function of scaling factor with initial

template molecule 1,3,4,5,6,10. e) Comparison modified multi scaling entropy genome, structural protein, template versus scaling factor with initial template=3.

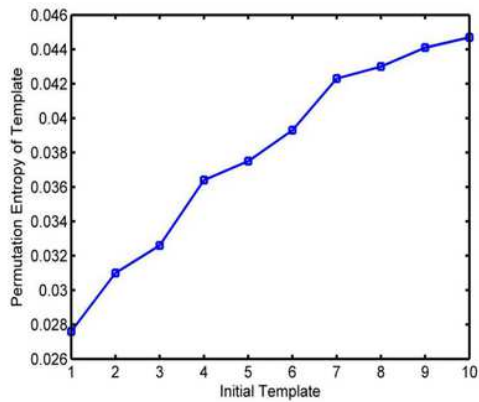


Figure.10.a

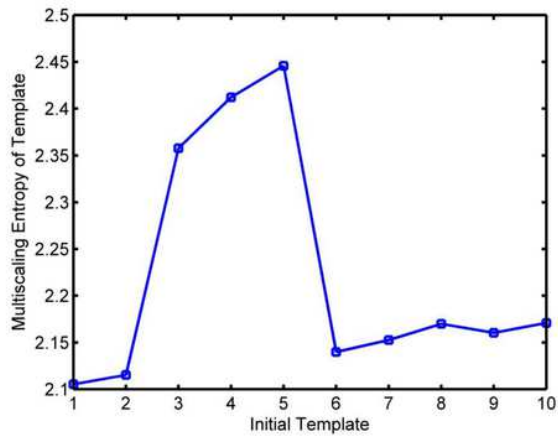


Figure.10.b

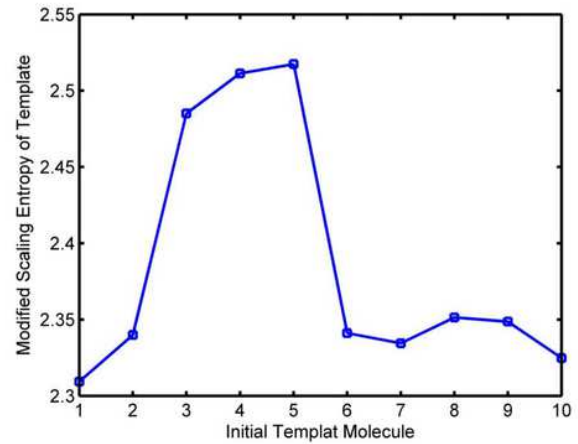


Figure.10.c

Figure 10

a) Permutation entropy of template versus initial template population b) Multiscaling entropy of template versus initial template population c) Modified multiscaling entropy of template versus initial template population